ACS ENVIRONMENTAL Au
AN OPEN ACCESS JOURNAL OF THE AMERICAN CHEMICAL SOCIETY

pubs.acs.org/environau

Perspective

Electrospun Nanofibrous Membranes for Controlling Airborne Viruses: Present Status, Standardization of Aerosol Filtration Tests, and Future Development

Hongchen Shen,* Minghao Han, Yun Shen, and Danmeng Shuai*

Cite This: *ACS Environ. Au* 2022, 2, 290–309

Read Online

ACCESS | Metrics & More | Article Recommendations

ABSTRACT: The global COVID-19 pandemic has raised great public concern about the airborne transmission of viral pathogens. Virus-laden aerosols with small size could be suspended in the air for a long duration and remain infectious. Among a series of measures implemented to mitigate the airborne spread of infectious diseases, filtration by face masks, respirators, and air filters is a potent nonpharmacologic intervention. Compared with conventional air filtration media, nanofibrous membranes fabricated via electrospinning are promising candidates for controlling airborne viruses due to their desired characteristics, i.e., a reduced pore size (submicrometers to several micrometers), a larger specific surface area and porosity, and retained surface and volume charges. So far, a wide variety of electrospun nanofibrous membranes have been developed for aerosol filtration, and they have shown excellent filtration performance. However, current studies using electrospinning for controlling airborne viruses vary significantly in the practice of aerosol filtration tests, including setup configurations and operations. The discrepancy among various studies makes it difficult, if not impossible, to compare filtration performance. Therefore, there is a pressing need to establish a standardized protocol for evaluating the electrospun nanofibrous membranes' performance for removing viral aerosols. In this perspective, we first reviewed the properties and performance of diverse filter media, including electrospun nanofibrous membranes, for removing viral aerosols. Next, aerosol filtration protocols for electrospun nanofibrous membranes were discussed with respect to the aerosol generation, filtration, collection, and detection. Thereafter, standardizing the aerosol filtration test system for electrospun nanofibrous membranes was proposed. In the end, the future advancement of electrospun nanofibrous membranes for enhanced air filtration was discussed. This perspective provides a comprehensive understanding of status and challenges of electrospinning for air filtration, and it sheds light on future nanomaterial and protocol development for controlling airborne viruses, preventing the spread of infectious diseases, and beyond.

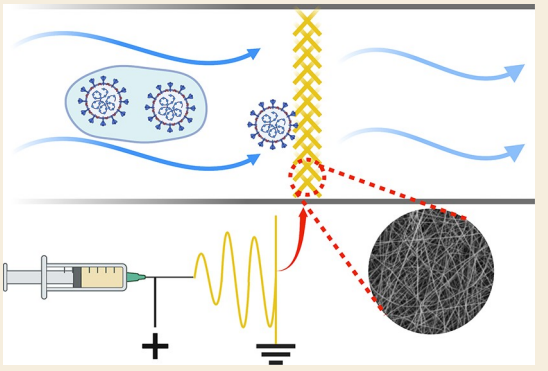

KEYWORDS: *electrospinning, viruses, aerosols, standardization, filtration tests*

1. INTRODUCTION

The global COVID-19 pandemic has raised serious public health concerns and economic losses since late 2019.[1] Besides transmission pathways through respiratory droplets, direct contact with an infected person, and indirect contact via fomites, mounting evidence has suggested that the airborne transmission of SARS-CoV-2, the viral pathogen causing COVID-19, is responsible for the fast and wide spread of the infectious disease.[2,3] The small size (aerodynamic diameters <100 μm) enables virus-laden aerosols to suspend in the air for a long duration.[4] SARS-CoV-2 RNA has been detected in aerosols sampled from two hospitals in Wuhan, China during the outbreak of COVID-19.[5] Moreover, SARS-CoV-2 possesses a half-life of 1.1 h in aerosols based on a lab study, which shows the persistence and potential infectivity of coronaviruses within aerosols.[6] In addition to SARS-CoV-2, a lot of viruses, e.g., measles virus, influenza virus, and Middle East respiratory syndrome coronavirus, are also confirmed to be air transmissible.[7] Nowadays, people spend most of their time staying in buildings whose confined indoor environments may further facilitate the spread of virus-laden aerosols. For example, the air movement generated by the heating, ventilation, and air conditioning (HVAC) systems increases

Received: October 28, 2021
Revised: February 26, 2022
Accepted: February 28, 2022
Published: March 11, 2022

https://doi.org/10.1021/acsenvironau.1c00047
ACS Environ. Au 2022, 2, 290–309

the travel distance of aerosols by preventing them from settling onto the ground or surfaces.[8,9]

It is widely accepted that physical barriers, e.g., face masks, respirators, and air filters, can mitigate the transmission of airborne viruses.[10] Face masks and respirators, especially surgical masks and N95 respirators, are confirmed to be effective measures in constraining the spread of COVID-19.[11] However, at the beginning of the COVID-19 pandemic, surgical masks and N95 respirators were once not readily available. The US Centers for Disease Control and Prevention (CDC) had to recommend the public to wear homemade cloth face masks rather than these strategic medical supplies which are intended for healthcare workers.[12] However, homemade cloth masks usually fail to achieve a satisfactory removal efficiency against viral aerosols.[13] In addition, most air filters for residential, commercial, and industrial buildings, e.g., air filters in HVAC systems, can only capture large airborne particles, e.g., dusts, mold spores, and bacteria, but not submicrometer viral aerosols.[14] Even though high-efficiency particulate air (HEPA) filters could be employed, their feasibility and wide application are always limited by the prohibitively high operational costs and energy consumption. Furthermore, most conventional face masks, respirators, and air filters are made of petroleum-based materials, e.g., polypropylene, which are not biodegradable and thus raise serious environmental concerns after disposal like plastic contamination.[15] Therefore, it is necessary to develop novel face masks, respirators, and air filters which can overcome the aforementioned challenges.

Electrospinning is a promising technique to produce nanofibrous membranes for controlling viral aerosols.[16,17] During electrospinning, dope solutions are stretched by a strong electric field (i.e., 1−5 kV cm^{-1}) and form nonwoven nanofibrous membranes. Compared with conventional air filtration media, the electrospun nanofibrous mats possess a reduced pore size (submicrometer to several micrometers), a larger specific surface area and porosity, and retained surface and volume charges, which enables a high viral aerosol filtration efficiency and a low pressure drop amid air filtration applications.[18] The development of miniaturized and portable electrospinning apparatuses further facilitates the wide applications of this technique for small-scale applications, e.g., personal tailored devices and manufacturing for small communities.[19] Moreover, the utilization of biodegradable polymeric materials in electrospinning mitigates the ever-increasing environmental concerns caused by plastic waste pollution.[20] So far, numerous studies have demonstrated the outstanding performance of electrospun membranes for removing airborne pathogens, including bacteria, fungi, and viruses from air streams.[21,22] Particularly, electrospun air filters fabricated in our previous study could remove up to 99.9% of coronavirus aerosols, which highlights the promising potential of electrospun membranes for controlling the airborne transmission of SARS-CoV-2 and beyond.[23]

Though many reviews and perspectives have discussed deploying electrospun nanofibrous membranes for air filtration applications, these studies are mainly focused on removing dusts, $PM_{2.5}$ and PM_{10}, and airborne bacteria.[24−28] Compared with other airborne pollutants, it is much more challenging to remove viral aerosols because the size of viral aerosols is much smaller and this size is within the size range of the most penetrating particles for mechanical air filtration (∼300 nm). In addition, considering that a low dose of airborne viruses can cause infections,[29] developing electrospun membranes with a high removal efficiency for removing viral aerosols is urgently needed. However, it is worth noting that current studies significantly vary in the practice of aerosol filtration tests, especially in terms of aerosol generation, filtration, collection, and detection. The discrepancy in the design of aerosol filtration experiments makes it difficult, if not impossible, to compare results across various studies. Therefore, it is necessary to establish standard protocols for evaluating the viral aerosol removal performance of electrospun membranes. In this perspective, the applications of air filtration in controlling airborne transmission of viruses, including common face masks, respirators, air filters, and electrospun membranes, were first reviewed. Next, important parameters which significantly influence the results of aerosol filtration tests were summarized. The standardized experimental protocol for evaluating the performance of electrospun membranes in removing viral aerosols was proposed. In the end, the future development of electrospun membranes for enhanced air filtration applications was discussed. This perspective advocates leveraging electrospinning for air filtration applications, particularly for controlling airborne pathogenic viruses; it promotes standardization of viral aerosol filtration tests; and it paves new avenues for better understanding and comparing the performance of removing viral aerosols by electrospun membranes from different studies.

2. AIR FILTRATION FOR CONTROLLING VIRAL AEROSOLS

2.1. Face Masks and Respirators

For comparison, the viral aerosol filtration performance of different commercially available face masks and respirators, i.e., surgical masks, N95 respirators, and face masks made from common fabrics, was reviewed. Generally speaking, under the regulation of 21 CFR 878.4040,[30] surgical masks are not designed for removing ultrafine viral aerosols.[31] The viral aerosol filtration performance of surgical masks is thus expected to be inferior to that of N95 respirators. N95 respirators must be certified by the National Institute for Occupational Safety and Health (NIOSH) which requires the tested respirators to achieve more than 95% of filtration efficiency against ultrafine aerosol particles. It is worth noting that in the certification tests, NaCl aerosol particles with an aerodynamic mass median diameter of 300 nm are utilized to challenge the respirators since 300 nm is considered as the most penetrating particle size (MPPS).[32] For mechanical filters without electric charges, the determination of MPPS of 300 nm is accurate. However, in the case of N95 respirators and surgical masks whose fibers are usually charged, MPPS shifts to smaller values, e.g., 50 to 100 nm.[33] Therefore, to avoid overestimating the performance of N95 respirators, aerosols with a wide size distribution should be used for testing the filtration efficiency. Basic cloth face masks are important alternatives to surgical masks and N95 respirators especially when the accessibility of these medical supplies is severely limited at the beginning of a pandemic.[34] However, unlike surgical masks and N95 respirators, no regulations are available for these face masks and it is important to understand their performance for stopping the airborne transmission of viruses.

For surgical masks and N95 respirators, the conclusions from different studies about their viral aerosol removal performance are quite controversial. Booth et al. tested the

https://doi.org/10.1021/acsenvironau.1c00047
ACS Environ. Au 2022, 2, 290−309

Table 1. Representative Studies of Face Masks and Respirators for Controlling Aerosols

ref	filtration media	performance	aerosol generation	filtration process	aerosol collection and detection
35	Surgical masks	Aerosol removal efficiency ranged from 9.09% to 98.2%.	Inert aerosol particles: generated from phosphate-buffered saline with 0.2% (w/v) bovine serum albumin; influenza virus aerosols	Dummy test head-based protocol	PortaCount Plus particle-counting device for inert particles; midget impingers with virus transport medium for viral aerosols
36	N95 respirators	At a flow rate of 85 L min^{-1}, the penetration of 30−70 nm NaCl aerosols might exceed 5%.	10−600 nm NaCl	Manikin-based protocol; two inhalation flow rates, 30 and 85 L min^{-1}	Wide range particle spectrometer
37	N95 respirators and surgical masks	Surgical masks were less efficient than N95 respirators; at a flow rate of 85 L min^{-1}, the penetration of MS2 aerosols might exceed 5%.	10−80 nm bacteriophage MS2 aerosols	Manikin-based protocol; two inhalation flow rates, 30 and 85 L min^{-1}	Wide range particle spectrometer
38	N95 respirators and surgical masks	N95 respirators were superior to surgical masks; one-third of tested N95 respirators failed to achieve the performance required by NIOSH.	40−1300 nm NaCl	Human subject-based protocol	Personal sampling system connected to an electrical low pressure impactor
39	Surgical masks and N95, N99 respirators	Filtration efficiency was higher than 97% for all tested masks.	Bacteriophage SM702 aerosols with an aerodynamic diameter of 0.744 μm	Manikin-based protocol	Aerodynamic particle sizer
40	32 cloth materials, surgical masks, and N95 respirators	No cloth materials possessed aerosol filtration performance comparable to that of N95 respirators.	50−825 nm NaCl	EN 1822 mask filtration protocol and ISO 29463 testing standard	Condensation particle counter
41	Cloth masks, common fabric materials, and N95 respirators	Masks made from common fabrics only provided limited protection against aerosol particles.	20−1000 nm NaCl	Two face velocities: 5.5 and 16.5 cm s^{-1}	TSI 8130 Automated Filter Tester (TSI 8130); TSI 3160 Fractional Efficiency Tester (TSI 3160)
42	Three types of cloth masks and one type of the surgical mask	The best cloth mask could remove up to 80−90% of polystyrene latex (PSL) aerosols which was comparable to the surgical mask.	Monodispersed PSL particles with a size of 30, 100, 500, 1000, and 2500 nm	Manikin-based protocol	Aerodynamic particle sizer; scanning mobility particle sizer
43	Household materials and surgical masks	The best material could achieve a viral aerosol filtration efficiency of 85.95% with a pressure drop of 10.18 Pa.	Bacteriophage MS2 aerosols	Henderson apparatus	Glass impingers with phosphate buffer
13	Household materials	Multiple layers of cloth masks were needed to achieve decent protection.	30 nm to 10 μm NaCl	Homemade filtration test system	Scanning mobility particle sizer, optical particle counter, condensation particle counter

https://doi.org/10.1021/acsenvironau.1c00047
ACS Environ. Au 2022, 2, 290−309

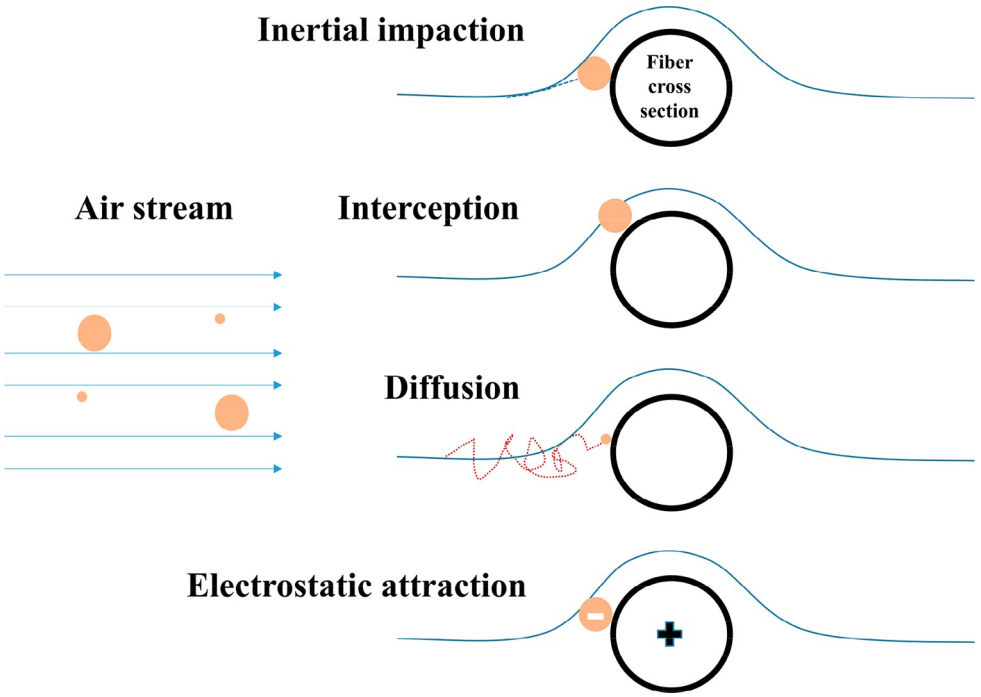

Figure 1. Mechanisms of electrospun nanofibrous membranes for removing aerosol particles from the air stream.

protective efficacy of surgical masks against both influenza virus aerosols and inert aerosol particles. Surgical masks from various sources possessed significantly different aerosol removal efficiencies, ranging from 9.09% to 98.2%, which demonstrated the limited protection provided by some surgical masks.[35] Bałazy et al. evaluated the filtration efficiency of N95 respirators against NaCl aerosol particles (10−600 nm). The results showed that the penetration of NaCl aerosol nanoparticles with certain sizes, i.e., 30−70 nm, at a high inhalation flow rate of 85 L min^{-1} might exceed 5% (the maximum penetration allowed by NIOSH certification for N95 respirators).[36] Bałazy et al. further challenged two models of N95 respirators and two models of surgical masks with MS2 virus aerosols of 10−80 nm. Again, under the high inhalation flow rate of 85 L min^{-1}, N95 respirators failed to achieve the required aerosol filtration efficiency, i.e., more than 95%. For surgical masks, the performance was even worse, i.e., more than 80% penetration of viral aerosols was observed.[37] Lee et al. determined the protection provided by surgical masks and N95 respirators against NaCl aerosol particles with bacterial and viral sizes (40−1300 nm). It was demonstrated that even though the average aerosol filtration efficiency of N95 respirators was 8 to 12 times better than that of surgical masks, about one-third of tested N95 respirators failed to achieve the performance required by NIOSH.[38] Wen et al. evaluated the protective performance of surgical masks and N95 and N99 respirators against bacteriophage SM702 aerosols with an aerodynamic diameter of 0.744 μm. Without considering mask fit, both surgical masks and N95 and N99 respirators showed promising viral aerosol removal efficacy, i.e., filtration efficiencies higher than 97% for all tested masks. However, the face fit factor test indicated that the surgical masks might not be able to provide sufficient protection against viral aerosols as N95 and N99 respirators did due to the lack of tight face seal.[39]

For basic cloth face masks, the aerosol removal efficiency is generally not comparable to medical grade masks, especially N95 respirators.[44] Zangmeister et al. measured the filtration efficiency and pressure drop of 32 cloth materials against NaCl aerosol particles with a diameter ranging from 50 to 825 nm. The surgical masks and N95 respirators were also investigated as the reference. The results indicated that no cloth materials possessed aerosol filtration performance comparable to that of N95 respirators which could achieve an average filtration efficiency of 99.9 ± 0.1% across the whole aerosol size range.[40] Rengasamy et al. tested the aerosol filtration efficiency of fabric materials from sweatshirts, T-shirts, towels, scarves, and cloth masks using both polydisperse and monodisperse NaCl aerosol particles. Compared with the N95 respirator, masks made from common fabrics only provided limited protection against aerosol particles.[41] Shakya et al. examined the aerosol filtration efficiency of four models of face masks, i.e., three types of cloth masks and one type of the surgical mask. In aerosol filtration tests, monodispersed polystyrene latex (PSL) particles with a size of 30, 100, 500, 1000, and 2500 nm were utilized. The best cloth mask could remove up to 80−90% of PSL aerosol particles, which was comparable to the surgical mask with a filtration efficiency of 78−94% but still worse than the reference N95 respirators.[45] Davies et al. examined the capacity of household materials and a surgical mask for capturing bacteriophage MS2 aerosols. Among all tested household materials, one vacuum cleaner bag showed the highest viral aerosol filtration efficiency of 85.95% with a pressure drop of 10.18 Pa. However, the surgical mask showed a better filtration efficiency of 89.52% and a lower pressure drop of 5.23 Pa.[43] Most recently, Drewnick et al. investigated the filtration efficiency of 44 household materials which might be used for constructing cloth masks against viral aerosols ranging from 30 nm to 10 μm. The performance of these materials was compared with that of surgical masks. The results indicated that multiple layers of cloth masks were needed to achieve decent protection against aerosol particles with a wide size distribution.[13] Representative studies of face masks and respirators for controlling aerosols are summarized in Table 1.

https://doi.org/10.1021/acsenvironau.1c00047
ACS Environ. Au 2022, 2, 290−309

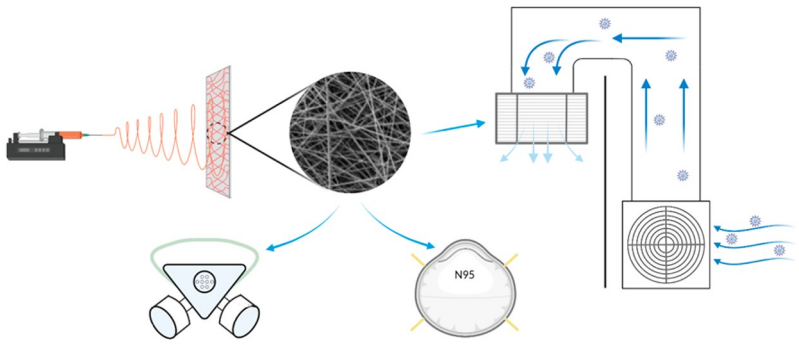

Figure 2. Applications of electrospun nanofibrous membranes for viral aerosol removal.

2.2. Air Filters for HVAC Systems

Without further functionalization or improvement, most air filters used in residential, commercial, and industrial buildings (minimum efficiency rating value (MERV) < 13) generally do not remove viral aerosols efficiently.[14] MERV, derived from the standardized air filtration test method ANSI/ASHRAE Standard 52.2−2017, represents an air filter's performance for removing airborne particles between 0.3 and 10 μm. The higher the MERV is, the better the air filter performs. Specifically, the air filter with a MERV of 13 could achieve at least 50%, 85%, and 90% of the removal efficiency for airborne particles with 0.3−1.0, 1.0−3.0, and 3.0−10.0 μm, respectively.[46] Huang et al. demonstrated that a low-efficiency HVAC air filter possessed poor performance against influenza virus A (H11N9) aerosols with a filtration efficiency of only 9.09%. Even combined with the nearby emission of unipolar air ions which could significantly enhance aerosol collection, the air filter only removed about 36% of viral aerosols.[47] Similarly, Hyun et al. improved the aerosol filtration performance of a mediocre air filter by charging the bacteriophage MS2 aerosols. At a face velocity of 0.3 m s^{-1}, charging MS2 aerosols improved the filtration efficiency from 56.5% to 63.5%.[48] Park et al. coated carbon nanotubes onto a glass fiber filter media by electro-aerodynamic deposition. At the face velocity of 0.2 m s^{-1}, the optimum modified air filter showed an enhanced filtration efficiency of 78.4% for bacteriophage MS2 aerosols compared with 54% of the pristine air filter.[49] Furthermore, Zhang et al. investigated the filtration performance of residential HVAC filters with different MERVs against MS2 aerosols. MERV 5, MERV 12, MERV 13, and MERV 14 showed an average viral aerosol filtration efficiency of 32%, 78%, 89%, and 97%, respectively.[50] HEPA filters are generally believed to provide the best protection against viral aerosols at the expense of their high pressure drop. With time passing by, the pressure drop keeps increasing with the accumulation of aerosol particles on the HEPA filters.[51] In some cases, however, even HEPA filters fail to efficiently remove viral aerosols. Heimbuch et al. pointed out that viable bacteriophage MS2 aerosols could penetrate two HEPA materials, i.e., Carbon HEPA Aerosol Canisters (CHACs) and the flat sheet HEPA material.[52] The penetrated viruses would finally lead to infections when susceptible hosts are exposed to sufficient viable virions.

2.3. Electrospun Nanofibrous Membranes

Electrospun nanofibrous membranes are able to capture virus-laden droplets and aerosols in the airstream by inertial impaction, interception, diffusion, gravitational settling, and electrostatic attraction (Figure 1).[53] A series of studies have thoroughly investigated the aerosol filtration mechanisms and readers are referred to these references.[34,54,55] Due to the reduced pore size, ultrafine fibers, and retained surface and volume charges, the electrospun nanofibrous membranes always possess a higher viral aerosol filtration efficiency compared with common face masks, respirators, and air filters available in the market.[23] In addition, the accessibility to surgical masks and N95 respirators is severely limited during every pandemic. Therefore, electrospun nanofibrous membranes with a high filtration efficiency for removing viral aerosols are promising alternatives to conventional personal protective equipment (PPE). Besides the filtration efficiency, pressure drop is another important index for assessing the filters' performance because the pressure drop is directly correlated with the breathability or energy consumption in the air filtration applications. For electrospun nanofibrous membranes, due to their high surface area to volume ratio, intuitively a high pressure drop is expected.[56] However, the enhanced porosity of electrospun nanofibrous membranes could reduce the pressure drop. Moreover, due to the slip effect, the drag force of air streams passing through electrospun nanofibrous membranes significantly decreases, further reducing the pressure drop in aerosol filtration.[57] Therefore, electrospun nanofibrous membranes always show a reduced pressure drop without compromising the filtration efficiency compared with many other filtration media. To simultaneously evaluate filtration efficiency and pressure drop of an electrospun nanofibrous membrane on the overall performance and fairly compare the performance with other filtration media, quality factor (QF) was proposed:

$$\mathrm{QF} = -\ln(1 - E)/\Delta P \quad (1)$$

where E is the aerosol filtration efficiency and ΔP is the pressure drop across the electrospun nanofibrous membranes

https://doi.org/10.1021/acsenvironau.1c00047
ACS Environ. Au 2022, 2, 290−309

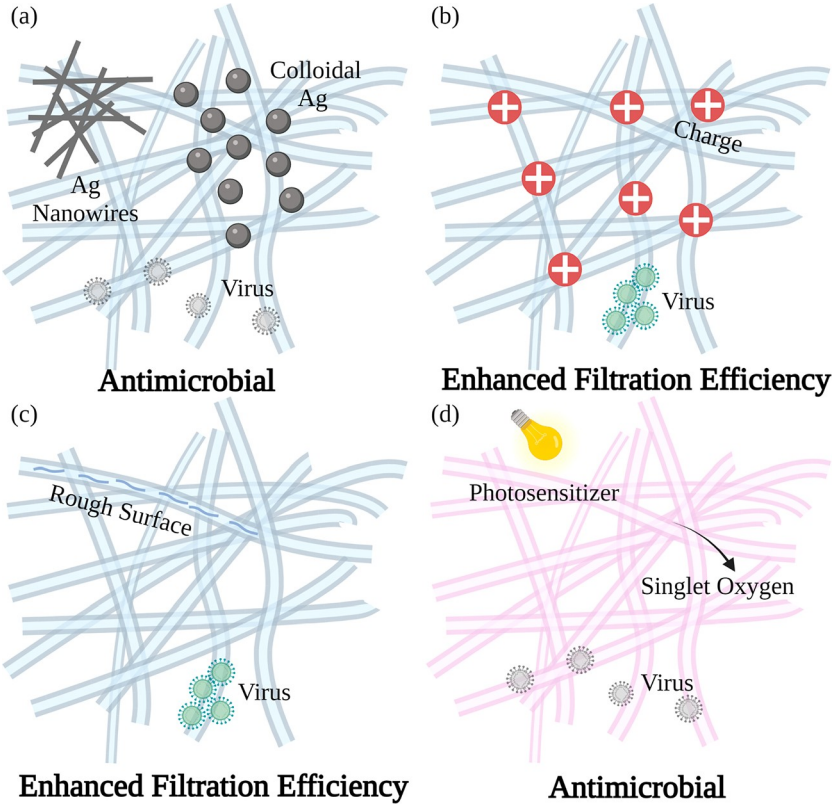

Figure 3. Schematics of functionalized electrospun nanofibrous membranes with enhanced performance for controlling airborne viruses. (a) Silver nanowires and nanoparticles deposited electrospun membranes with the antimicrobial function,[21,61] (b) an electrostatically charged electrospun polyvinylidene difluoride (PVDF) membrane showing an enhanced aerosol filtration efficiency,[16] (c) an electrospun polyacrylonitrile (PAN) membrane with an increased roughness for better capturing viral aerosols,[63] and (d) a rose bengal photosensitized electrospun PVDF membrane generating singlet oxygen for inactivating viral aerosols under light exposure.[64] Green and gray color labeled viruses represent live and dead viruses, respectively.

amid the aerosol filtration. A higher QF generally indicates better aerosol filtration performance.

So far, a wide range of electrospun nanofibrous membranes have been developed for aerosol filtration applications, and most of them exhibit promising performance. These electrospun membranes could be used as PPE and indoor air filters for viral aerosol removal (Figure 2). Specifically, Matulevicius et al. fabricated electrospun filter media from polyamide 6 (PA6), polyamide 6/6 (PA6/6), polyvinyl acetate (PVAc), polyacrylonitrile (PAN), and cellulose acetate (CA). The product membranes were challenged by monodisperse PSL (100 and 300 nm) and NaCl (6 to 1000 nm) aerosol particles and PVAc membranes showed the best aerosol filtration performance, i.e., QF = 0.0548 Pa^{-1} (E = 98.8% and ΔP = 80.6 Pa).[18] Chattopadhyay et al. electrospun CA into a series of air filters with various fiber diameters (0.1 to 1 μm), solidities (0.1 to 0.2), and thicknesses (7 to 51 μm). The product membranes along with two commercial air filters, i.e., a glass fiber filter and a CA microfiber filter, were challenged by one solid aerosol (NaCl) and one liquid aerosol (di(2-ethylhexyl) sebacate (DEHS)). Compared with the commercial air filters, the electrospun nanofibrous membranes showed better aerosol filtration performance.[56] Zhang et al. demonstrated that electrospun nanofibrous PAN mats had the highest QF of 0.0297 Pa^{-1} in aerosol filtration tests, which was comparable to two commercial HEPA filters with a QF of 0.00752 and 0.0304 Pa^{-1}. In addition, they found that instead of increasing the thickness of electrospun nanofibrous membranes, better aerosol filtration performance was achieved by stacking multiple layers of thin electrospun mats.[58] By increasing the conductivity of the electrospinning dope solution, Balgis et al. synthesized bead-free nanofibrous PAN air filters with the fiber diameter less than 100 nm. The aerosol filtration performance of the electrospun air filters was evaluated by using monodispersed NaCl aerosol particles (100 nm). It is worth noting that due to the slip effect, the pressure drop of product air filters amid aerosol filtration tests did not significantly increase as predicted by the theory.[59] Hung et al. fabricated PA6 electrospun nanofibrous air filters with the diameter of 94 and 185 nm, respectively. It was demonstrated that the aerosol filtration performance of the air filters, evaluated by QF, was dependent on the size distribution of the challenging aerosol particles. The electrospun nanofibrous filter with a fiber diameter of 185 nm showed better performance for removing 50−90 nm NaCl aerosol particles, but the electrospun nanofibrous filter with 94 nm fibers removed NaCl aerosol particles ranging from 100−380 nm more effectively.[60] Furthermore, in our previous study, electrospun polyvinylidene difluoride (PVDF) air filters were challenged by both NaCl and coronavirus aerosols (generated from murine hepatitis virus A59 (MHV-A59)).[23] The electrospun nanofibrous mats could remove up to 99.9% of coronavirus aerosols, which outperformed a surgical mask and two cloth masks.

To achieve enhanced aerosol filtration efficiency and more desirable characteristics, such as the antimicrobial capacity, the pristine electrospun membranes are further tailored and

https://doi.org/10.1021/acsenvironau.1c00047
ACS Environ. Au 2022, 2, 290−309

Table 2. Representative Studies of Electrospun Nanofibrous Membranes and Reference Filtration Media for Controlling Aerosols

ref	membrane	membrane characteristics	performance QF and (E)	aerosol generation	filtration process	aerosol collection and detection
16	Charged PVDF[a] filters	Four filters with an average fiber diameter of 84, 191, 349, and 525 nm, respectively	QF of all filters exceeded 0.0768 Pa^{-1} (90%); QF was calculated based on 100 nm aerosol particles.	50−500 nm NaCl	Aerosols passing through a dryer and a neutralizer; face velocity of 5.3 cm s^{-1}	Condensation particle counter
17	Herbal extract incorporated PVP[b] nanofibers	Mean fiber diameter of 470 nm	QF: 0.198 Pa^{-1} (99.99%); 99.98% antimicrobial activity	*S. epidermidis* bioaerosols with a geometric mean diameter of 0.84 μm	Aerosols passing through a dryer and a neutralizer; face velocity of 1.79 cm s^{-1}	Aerodynamic particle sizer
18	PVAc[c]	Beaded fibers; mean fiber diameter of 235 ± 65 nm; basis weight of 11.34 ± 0.40 g m^{-2}	QF: 0.0548 Pa^{-1} (98.8%) QF: 0.0427 Pa^{-1} (96.8%)	100 nm PSL[e] 300 nm PSL	Aerosols passing through a dryer and a charge equalizer; face velocity of 5.3 cm s^{-1}	Electrical low pressure impactor (detection limit of 6 nm to 10 μm)
	PAN[d]	Uniform fibers; mean fiber diameter of 535 ± 55 nm; basis weight of 5.26 ± 0.31 g m^{-2}	QF: 0.0433 Pa^{-1} (98.0%) QF: 0.0352 Pa^{-1} (95.8%)	100 nm PSL 300 nm PSL		
23[f]	$PVDF_{20}$	Mean fiber diameter of 300 nm; mean flow pore size of 2.7 μm	QF: 0.0911 Pa^{-1} (98.8%) for removing NaCl aerosols; QF: 0.0971 Pa^{-1} (99.1%) for removing murine hepatitis virus A59 (MHV-A59) aerosols	NaCl and MHV-A59 aerosols with the most dominant aerosol size of 420−450 nm	Face velocity of 5.3 cm s^{-1}	Impinger filled with deionized water and phosphate-buffered saline for collecting NaCl and MHV-A59 aerosols, respectively; ion chromatography and a reverse transcription-quantitative polymerase chain reaction for quantifying NaCl and MHV-A59, respectively
	$PVDF_{30}$	Mean fiber diameter of 300 nm; mean flow pore size of 2.4 μm	QF: 0.173 Pa^{-1} (99.99%) for removing NaCl aerosols; QF: 0.121 Pa^{-1} (99.9%) for removing MHV-A59 aerosols			
	$PVDF_{20}$/PEI	Mean fiber diameter of 400 nm; mean flow pore size of 2.1 μm	QF: 0.00788 Pa^{-1} (90.3%) for removing NaCl aerosols; QF: 0.0159 Pa^{-1} (99.1%) for removing MHV-A59 aerosols			
	$PVDF_{20}$/PVPA	Mean fiber diameter of 500 nm; mean flow pore size of 1.7 μm	QF: 0.0282 Pa^{-1} (92.8%) for removing NaCl aerosols; QF: 0.0337 Pa^{-1} (95.7%) for removing MHV-A59 aerosols			
	Surgical mask	Mean fiber diameter of 5.7 μm; mean flow pore size of 17.5 μm	QF: 0.152 Pa^{-1} (89.7%) for removing NaCl aerosols; QF: 0.269 Pa^{-1} (98.2%) for removing MHV-A59 aerosols			
	Cotton mask	Mean fiber diameter of 11.1 μm; mean flow pore size of 45.7 μm	QF: 0.0520 Pa^{-1} (54.0%) for removing NaCl aerosols; QF: 0.0884 Pa^{-1} (73.3%) for removing MHV-A59 aerosols			
	Neck gaiter	Mean fiber diameter of 12.0 μm; mean flow pore size of 102.1 μm	QF: 0.153 Pa^{-1} (31.6%) for removing NaCl aerosols; QF: 0.240 Pa^{-1} (44.9%) for removing MHV-A59 aerosols			
58	PAN single layer	Mean fiber diameter of 224 nm	QF: 0.0370 Pa^{-1} (47.7%)	300 nm PSL	Aerosols passing through a dryer; face velocity of 5.3 cm s^{-1}	Scanning mobility particle sizer
	PAN triple layers	Mean fiber diameter of 224 nm	QF: 0.0618 Pa^{-1} (92.1%)			
	Millipore glass fiber HEPA filter	1.0 μm pore size, hydrophilic glass fiber with binder resin, 47 mm diameter	QF: 0.00752 Pa^{-1} (99.99%)			
	LydAir MG high alpha HEPA filter	N/A[g]	QF: 0.0304 Pa^{-1} (99.98%)			
62	Tetraethyl orthosilicate (12 wt	Mean fiber diameter of 2039 nm and mean pore size of 2.7 μm	QF: 0.0325 Pa^{-1}	Polydisperse KCl	Relative humidity below 65%; face	Particle counters TSI 9306−03

https://doi.org/10.1021/acsenvironau.1c00047
ACS Environ. Au 2022, 2, 290−309

Table 2. continued

ref	membrane	membrane characteristics	performance QF and (E)	aerosol generation	filtration process	aerosol collection and detection
	%) doped PAN membranes				velocity of 5, 10, 15 cm s^{-1}	
64	Photosensitized PVDF membrane	Mean fiber diameter of 200 nm; mean flow pore size of 1.5 μm	QF: 0.0526 Pa^{-1} (99.1%) for removing NaCl aerosols; QF: 0.0539 Pa^{-1} (99.2%) for removing MHV-A59 aerosols	NaCl and MHV-A59 aerosols with the most dominant aerosol size of 420−450 nm	Face velocity of 5.3 cm s^{-1}	Impinger filled with deionized water and phosphate-buffered saline for collecting NaCl and MHV-A59 aerosols, respectively; ion chromatography and a reverse transcription-quantitative polymerase chain reaction for quantifying NaCl and MHV-A59, respectively
65	PAN/PAA[h]	Mean fiber diameter of 366 nm; average pore size of 44.4 nm	QF: 0.0608 Pa^{-1} (99.99%)	300−500 nm NaCl	Face velocity of 5.3 cm s^{-1}	Automated filter tester
66	PET[i]	Randomly oriented fibers; fibers electrospun from 10 wt % PET with an average diameter of 480 nm	Pristine PET electrospun membranes with better filtration efficiency for removing $PM_{2.5}$; PET membranes treated by *N*-methyl-2-pyrrolidone with better filtration performance for removing the green fluorescent protein monoclonal antibody (eGFP)	$PM_{2.5}$ aerosols generated by burning a moxa stick	Face velocity of 3 m s^{-1}	An air quality monitoring system
	PET			Viral aerosols simulated by eGFP		A Petri dish used to collect penetrated eGFP; a phase contrast light microscopy used for detecting eGFP
67	PEO[j]	Mean fiber diameter of 208 nm	0.0159 Pa^{-1} (92.5%) for 300 nm particles	Polydisperse NaCl	Aerosols passing through a dryer and a neutralizer; face velocity of 5.0 cm s^{-1}	Condensation particle counter
68	CA[k] modified with cetylpyridinium bromide surfactant	Mean fiber diameter of 239 nm	Filtration efficiency was almost 100%.	Polydisperse NaCl	Aerosols passing through a dryer and a neutralizer; face velocity of 1.6 cm s^{-1}	Scanning mobility particle sizer

[a]Polyvinylidene difluoride (PVDF). [b]Polyvinylpyrrolidone (PVP). [c]Polyvinyl acetate (PVAc). [d]Polyacrylonitrile (PAN). [e]Polystyrene latex (PSL). [f]In the ref 23, $PVDF_{20}$ and $PVDF_{30}$ are membranes fabricated via 20 and 30 min of electrospinning, respectively. $PVDF_{20}$/PEI and $PVDF_{20}$/PVPA are $PVDF_{20}$ membranes coated with poly(ethylenimine) (PEI) and poly(vinylphosphonic acid) (PVPA), respectively. [g]N/A: Data not available. [h]Polyacrylonitrile/poly(acrylic acid) (PAN/PAA, with the weight ratio of 6/4). [i]Poly(ethylene terephthalate (PET). [j]Poly(ethylene oxide) (PEO). [k]Cellulose acetate (CA).

https://doi.org/10.1021/acsenvironau.1c00047
ACS Environ. Au 2022, 2, 290−309

Table 3. Selected Standardized Air Filtration Test Methods

designation	title	content provider
British Standard 3928:1969	Method for sodium flame test for air filters (other than for air supply to I.C. engines and compressors)	British Standards Institution
EN 149:2001+A1:2009	Respiratory protective devices - Filtering half masks to protect against particles - Requirements, testing, marking	European Committee for Standardization
EN 1822-1:2009	High efficiency air filters (EPA, HEPA and ULPA[a])—part 1: classification, performance testing, marking	European Committee for Standardization
ASTM F3502-21	Standard specification for barrier face coverings	American Society for Testing and Materials
ASTM F2299/F2299M-03(17)	Standard test method for determining the initial efficiency of materials used in medical face masks to penetration by particulates using latex spheres	American Society for Testing and Materials
ASTM F2100-21	Standard specification for performance of materials used in medical face masks	American Society for Testing and Materials
42 CFR84.174	Filter efficiency level determination test - nonpowered series N, R, and P filtration	National Institute for Occupational Safety and Health
ANSI/ASHRAE Standard 52.2-2017	Method of testing general ventilation air-cleaning devices for removal efficiency by particle size	American Society of Heating, Refrigerating and Air-Conditioning Engineers

[a]Ultralow penetration air filters (ULPA).

functionalized. Park et al. electrosprayed silver nanowires onto the surface of electrospun PAN mats (Figure 3a). Silver nanowires not only improved the electrospun membranes' filtration efficiency against bacterial and viral aerosols but also exhibited potent antiviral efficacy. In particular, 72.5% of bacteriophage MS2 were inactivated after the 30 min of aerosol filtration test.[61] Similarly, Blosi et al. obtained silver nanoparticles loaded poly(vinyl alcohol) (PVA) nanofibers by electrospinning the dope solution containing colloidal silver and PVA (Figure 3a). The product membranes were able to capture 97.7% of nanosized aerosol particles (10−700 nm), which meets the EN149−2009 standard.[21] To enhance the filtration efficiency against fine viruses and other air pollutants, Leung et al. electrostatically charged the electrospun PVDF fibers using corona discharge (Figure 3b). The charged nanofibrous filters were challenged by NaCl aerosol particles with the size of 50−500 nm. In this study, special attention was paid to the aerosol size at 100 nm which is the mean size of SARS-CoV-2 (60−140 nm). The tailored electrospun air filters could capture more than 90% of 100 nm aerosol particles with a pressure drop less than 30 Pa.[16] Al-Attabi et al. fabricated wrinkled electrospun nanofibrous membranes by incorporating tetraethyl orthosilicate into the PAN dope solution. The wrinkled structure offered the membrane a highly effective surface for capturing aerosols and an enlarged pore size to reduce the pressure drop. As a result, the composite electrospun nanofibrous membranes showed a superior KCl aerosol filtration performance when compared with a commercial glass fiber filter.[62] Similarly, Wang et al. modified the roughness of electrospun nanofibrous membranes by incorporating silica nanoparticles into the PAN dope solution (Figure 3c). Compared with the pristine PAN membranes, the composite membranes possessed a reduced fiber diameter and pore size, but an enhanced porosity, pore volume, and surface area. In aerosol filtration tests, the optimum composite membranes exhibited a better performance with a QF of 0.0308 Pa^{-1} than the pristine PAN air filter with a QF of 0.0218 Pa^{-1}.[63] We also synthesized one photosensitive nanofibrous air filter by incorporating photoreactive dyes, e.g., rose bengal, into electrospun PVDF membranes (Figure 3d). The product membranes could capture 99.2% of MHV-A59 aerosols. Moreover, under the irradiation of visible light, like from a desk lamp, the photosensitized nanofibrous membranes could inactivate 97.1% of MHV-A59 in virus-laden droplets within 15 min.[64] Representative studies of electrospun nanofibrous membranes and reference filtration media for controlling aerosols are summarized in Table 2.

3. STANDARDIZATION OF AEROSOL FILTRATION TESTS FOR ELECTROSPUN NANOFIBROUS MEMBRANES

So far, a wide variety of standardized test methods have been proposed for evaluating the filtration performance of face masks, respirators, and air filters (Table 3). These standardized test methods, however, are rarely directly employed in laboratory studies, which could be attributed to the limited access to the special facilities and the incapacity of standardized test methods for meeting specific requirements. With ANSI/ASHRAE Standard 52.2−2017 taken as an example, the standard requires a specially designed test duct which is at least 5 m in length. In addition, this method utilizes polydisperse solid-phase (dry) potassium chloride particles to test the filtration efficacy of filters, which does not always simulate the performance of viral aerosol removal.[46] As reviewed in section 2, researchers usually utilize customized aerosol filtration test systems to investigate the filtration performance of face masks, respirators, and air filters. Therefore, aerosol filtration test methods from different studies vary in aerosol generation, filtration, collection, and detection, which could significantly influence the final results. For electrospun nanofibrous membranes, to accurately compare aerosol filtration results from various studies, a standardized aerosol filtration test protocol should be implemented.

In this section, important operating parameters, e.g., the face velocity of aerosols passing through electrospun nanofibrous membranes, and methods, e.g., collection and detection of aerosols, in the aerosol filtration tests are first discussed. In the end, a standardized aerosol filtration system is proposed.

3.1. Aerosol Generation

3.1.1. Aerosol Origin. Most viral aerosol related studies utilize surrogate aerosol particles to evaluate the filtration performance due to the biosafety concern caused by the aerosolization of virulent pathogens. The surrogate aerosol particles include both nonbiological particles, e.g., NaCl and PSL, and biological particles, e.g., bacteriophage MS2. Compared with pathogenic viruses, biological aerosol surrogates, i.e., bacteriophage or animal virus, could not cause human infection, and hence they are safe to work with. Several studies compared the performance of both nonbiological and biological aerosol surrogates in the filtration

https://doi.org/10.1021/acsenvironau.1c00047
ACS Environ. Au 2022, 2, 290−309

tests. The results confirmed the feasibility of utilizing nonbiological surrogates to assess the filtration efficacy.[23,69,70] However, special attention should be paid when someone tries to interpret filtration data retrieved from nonbiological surrogates due to the huge differences in physical and chemical properties between these surrogates and human pathogenic viruses. For example, it has been demonstrated that both aerosol size and morphology significantly affect the filtration efficiency.[70] Fungi and bacteria within aerosols may aggregate to form pairs, chains, or clusters, which impart irregular shapes and surface structures to aerosol particles.[71] In contrast, nonbiological surrogates, like DEHS liquid oily particles and PSL, are in perfectly spherical shape and always possess a smooth surface. It has been demonstrated that these structural differences finally result in various aerosol collection efficiencies.[72] Similarly, the discrepancy in the air filters' filtration efficiency for bacterial aerosols and conventional nonbiological aerosol surrogates was also observed. In a study, bacterial aerosols and mineral dusts had the same aerodynamic diameter, but bacterial aerosols exhibited various morphologies.[70] Though similar studies on viral aerosols are limited, evidence did show that under some circumstances, like bacteria and fungi, viruses could aggregate inside the aerosol particles.[73] In addition, when aerosolized from solutions rather than deionized (DI) water, viruses within aerosols adhere to nonvolatile components, e.g., salts and proteins, after water evaporation (section 3.1.2). These composite solid particles may possess increased sizes and a more irregular morphology, which makes nonbiological aerosol surrogates difficult to mimic. As a conclusion, in aerosol filtration tests, the best candidates for aerosol generation are viruses of interest, such as influenza virus A. When the aerosolization of the target virus is highly risky, e.g., SARS-CoV-2, surrogate aerosols should be employed. Moreover, compared with nonbiological surrogates, viral surrogates of bacteriophages and animal viruses that closely mimic the virus of interest may help better understand the performance of face masks, respirators, or air filters against pathogenic viral aerosols.

Some viral surrogates used in the aerosol studies along with their structural features and hosts are summarized in the Table 4. As reviewed, the surrogate viruses have diverse morphologies, sizes, and structures, which makes them perfect substitutes for pathogenic viruses. In aerosol filtration tests, viral surrogates possess a similar structural feature to pathogenic viruses should be first considered. For example, MHV-A59, a β-coronavirus that shares a similar diameter and structure with SARS-CoV-2, was used in authors' previous studies to evaluate the aerosol filtration efficiency of electrospun nanofibrous membranes.[23,64]

3.1.2. Media for Aerosolization. In aerosol filtration, the atomization method is generally utilized to produce challenge aerosols. During atomization, liquid containing surrogates or pathogenic viruses is broken into droplets and aerosols.[55] For nonbiological surrogates, DI water is always selected as the solvent to prepare the solutions or suspensions for aerosol generation. For viruses, however, a series of solvents such as water or artificial saliva may be used to accommodate viral particles. This section is mainly focused on the influence of different aerosolization media on viral aerosols.

It has been demonstrated that the media for aerosolization significantly influence the size distribution, composition, and viral viability of the produced viral aerosols. Zuo et al. generated bacteriophage MS2 aerosols with human saliva, artificial saliva, and cell culture medium (tryptic soy broth, TSB). The results indicated that the size distribution of aerosol particles achieved from different suspensions significantly varied. Specifically, the size distribution of aerosols by particle number from TSB was log-normal, while that from human saliva was bimodal. It is worth noting that the size distributions of aerosol particles by volume and by number were totally different in this study. The virus size distribution, i.e., viral infectivity as a function of their carrier particle size, better followed the pattern of aerosol size distribution by volume. Moreover, the viability of aerosolized MS2 from TSB and artificial saliva was higher than that from human saliva.[79,80] Pan et al. utilized DI water, artificial saliva, and a beef extract solution as the media to generate bacteriophage MS2 aerosols. The aerosol size distribution and virus size distribution were determined after aerosols passed through a dilution dryer where the moisture was removed. Compared with aerosols generated from DI water, both aerosol particle number and count mode (peak number in the aerosol particle size distribution) generated from artificial saliva and the beef extract solution increased. This is because, besides MS2, aerosols from artificial saliva and the beef extract solution also contained other solid components such as mucin proteins. The results also showed the enhanced viability of MS2 in artificial saliva after aerosolization compared with DI water and the beef extract solution, which confirmed the protective effect of artificial saliva for aerosolized MS2.[73] Similarly, Smither et al. investigated the viability of aerosolized SARS-CoV-2 in tissue culture media and artificial saliva. It is found that under the same aerosolization conditions, fewer aerosols were generated from artificial saliva than from tissue culture media. Moreover, viability of SARS-CoV-2 in aerosols generated from artificial saliva decayed more slowly at a higher relative humidity (RH) but more rapidly at a medium RH than that in aerosols generated from tissue culture media.[81] For the viral aerosol composition, Stiti et al. has confirmed that nonspherical solid residues were left after water evaporation for viral aerosols generated from saliva. Besides viruses, the aerosols may also contain electrolytes, inorganic salts, human cells, and

Table 4. Virus Surrogates Used in Aerosol Studies

virus surrogates	host	structural features	ref
Murine hepatitis virus A59	HeLa-mCC1a cells	~85 nm in diameter, spherical, enveloped	23
Bacteriophage MS2	*Escherichia coli* (*E. coli*)	~25 nm in diameter, spherical, nonenveloped	37
Bacteriophage SM702	*Serratia marcescens*	Isometric polyhedral head of ~64 nm in diameter, with a tail of ~143 nm in length	74
Bacteriophage F2	*E. coli*	30−100 in diameter, spherical, nonenveloped	74
Bacteriophage ϕX174	*E. coli*	~25 nm in diameter, spherical, nonenveloped	75
Bacteriophage P008	*Lactococcus lactis*	Isomeric capsid of 53 nm in diameter, with a tail of ~159 nm in length	75
Bacteriophage T3	*E. coli*	Spherical head with a diameter of ~45 nm, with a short tail	76
Bacteriophage ϕ6	*Pseudomonas syringae*	~85 nm in diameter, spherical, enveloped	42
Bacteriophage PR772	*E. coli*	~82 nm in diameter, spherical, nonenveloped	77
Bacteriophage PM2	*Pseudoalteromonas espejiana*	~60 nm in diameter, spherical, nonenveloped	78

https://doi.org/10.1021/acsenvironau.1c00047
ACS Environ. Au 2022, 2, 290−309

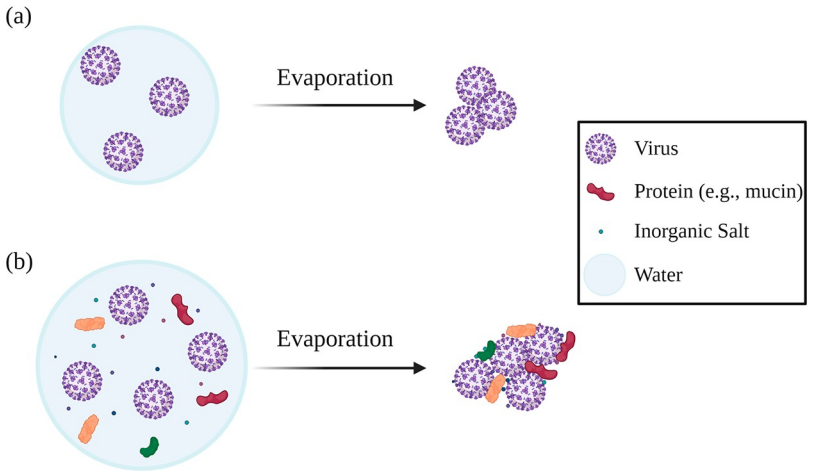

Figure 4. Viral aerosols generated from (a) deionized water and (b) biological solvents like saliva. Viral aerosols generated from biological solvents dry in a low humidity environment, and viruses are protected by nonvolatile components like inorganic salts and mucin proteins after water evaporation.

proteins.[82] With the aid of scanning electron microscopy, Woo et al. visualized the filtering facepiece respirators which were contaminated by MS2 aerosols generated from DI water, the beef extract solution, and artificial saliva. The collected dried aerosols on the surface of respirators significantly varied in morphology. For aerosols generated from DI water, naked MS2 aggregates were observed on the substrate. For aerosols generated from artificial saliva and the beef extract solution, however, MS2 aggregates were embedded in other solid components in the solutions, e.g., mucin.[83] The influence of media on the generated viral aerosols was depicted in the Figure 4.

3.1.3. Aerosol Size. The filtration performance of face masks, respirators, and air filters is highly dependent on the aerosol size. Generally, the size of virus-laden particles spans a wide range from submicrometers to hundreds of micrometers. Johnson et al. demonstrated that size distributions of human-expired aerosols varied depending on activities and aerosol generation processes. Specifically, speaking generated a particle size distribution with three count modes at 1.6, 2.5, and 145 μm, which resulted from the aerosol formation from the lower respiratory tract, larynx, and upper respiratory tract, respectively.[84] Wang et al. demonstrated the presence of influenza A RNA in aerosols sampled under different scenarios. The results indicated that more than 60% of viral genome copy numbers were associated with aerosol particles with a size less than 2.5 μm. However, in their study, the infectivity of influenza A within the aerosols was not quantified.[29] Yan et al. verified the presence of the influenza viral genome in both small (<5 μm) and large (>5 μm) aerosols exhaled from infected patients. In addition, they further successfully recovered infectious influenza viruses from fine aerosols (<5 μm), which confirmed the possibility of airborne transmission of the disease.[85] Given the ultrafine fibers and small pore size, electrospun nanofibrous membranes always achieve a high filtration efficiency for large droplets (defined as particles with the size >100 μm in this perspective). Therefore, fine aerosol particles with a diameter less than 100 μm, especially aerosols with submicrometer diameters, should be utilized to challenge the target electrospun nanofibrous membranes. However, it is worth noting that the virus-laden aerosols are never smaller than a single naked virus. Sometimes enlarged viral aerosols are observed due to the aggregation of viral particles and solid components (as reviewed in section 3.1.2) within the aerosols. Therefore, in aerosol filtration tests for removing viruses, the lowest limit of the aerosol size that should be considered equals the size of the target virus, e.g., ~25 nm for bacteriophage MS2, or ~100 nm for SARS-CoV-2. In the end, it should be noted that aerosol sizes characterized by various techniques may be different. For example, Sanchez et al. measured the size distribution of submicrometer and supramicrometer aerosols using a scanning mobility particle sizer (SMPS) and an aerodynamic particle sizer (APS), respectively.[86] Since SMPS and APS utilize different principles, i.e., electrical mobility and time-of-flight, respectively, to determine the aerosol particle size, each instrument has an optimal range for aerosol size characterization (2.5−1000 nm for SMPS vs 0.5−20 μm for APS).[55,87] To combine aerosol size spectra retrieved from two distinct instruments, a proper conversion is needed. For example, Khlystov et al. developed an algorithm for fitting APS data to SMPS data.[88]

3.1.4. Aerosol Charge. Aerosol particles, no matter whether they are derived from nonbiological sources or viruses, are charged after aerosolization. For example, both *Pseudomonas fluorescens* and NaCl aerosols with the same size generated by a Collison nebulizer showed a bipolar charge distribution. Compared with NaCl, the bacterial aerosols (with a net negative charge) had a much wider charge distribution with the highest charge of 13,000 elementary charges, while NaCl aerosols only carried tens of elementary charges.[89] In addition, Hogan et al. found that MS2 aerosols produced by a Collison nebulizer and a stainless steel atomizer carried an average of −0.91 and −0.14 elementary charges, respectively. The discrepancy was attributed to the different electrical properties of the construction materials between the nebulizer and the atomizer (glass versus stainless steel). In this study, agglomerates of MS2 viruses were observed in the aerosols. Interestingly, after aerosols passing through the Po-210 bipolar charger (a charge neutralizer) which reduced charges carried by the aerosols, the agglomerates of MS2 viruses broke apart into ultrafine viral particles. Therefore, it seems that the charge carried by the aerosols can indirectly affect the aerosol filtration efficiency by tailoring the aerosol size.[90]

https://doi.org/10.1021/acsenvironau.1c00047
ACS Environ. Au 2022, 2, 290−309

The charge carried by viral aerosols also directly influences the filtration performance. Electrostatic interactions between aerosol particles and the filter media play a dominant role in determining the aerosol filtration efficiency of face masks, respirators, and air filters, especially for viral aerosols with a size of submicrometers. Electrostatic attractions come from several sources and enhance the aerosol filtration efficiency.[91] If aerosol particles and the filter media are oppositely charged, the Coulombic forces pull aerosol particles to the filter media. If only aerosol particles or the filter media carry charges, dielectrophoretic forces between aerosol particles and the filter media make them attract each other.[55] However, the electrostatic repulsions between the same charged aerosol particles and the filter media may reduce the filtration efficiency.[92] Chen et al. investigated the effects of charge carried by aerosol particles on the filtration efficiency of a filter facepiece respirator and found that charged aerosol particles always showed a reduced penetration. Moreover, the results indicated that the influence induced by the charge was more significant on the aerosols with small sizes. It has also demonstrated that a slight shift in the charge state of aerosol particles could result in an obvious variation in aerosol filtration results.[93] Moyer et al. challenged a series of filter media with both neutralized and non-neutralized silica dusts, lead fumes, and dioctyl phthalate (DOP) aerosols, respectively. The results indicated that the largest enhancement, i.e., 4−11%, of the filtration efficiency was observed for the charged DOP aerosols compared with the neutralized aerosols. However, it should be noted that for silica dusts and lead fumes, the charged aerosols did not always mean an enhanced filtration efficiency.[94] In addition, Drewnick et al. also found that the aerosol charge could enhance the filtration efficiency especially when the air filters also carried charges.[13] Therefore, to eliminate the uncertainty caused by the aerosol charge and to better compare the aerosol filtration results from different studies, the aerosols generated should pass through a neutralizer, e.g., a radioactive ionizer.[95] After neutralization, the aerosol charge (with zero net charge) could be described by Boltzmann statistics.

3.2. Aerosol Filtration

3.2.1. Face Velocity. The face velocity at which the challenge aerosol particles pass through the filtration media determines both the filtration efficiency and the pressure drop. Generally, at large face velocities, aerosol collection caused by impaction is enhanced due to the higher inertia of aerosols while the collection efficiency of diffusion and electrostatic attraction decreases because of the shorter retention time of air flow in the filtration media.[13,93] Since diffusion and electrostatic attraction are dominant filtration mechanisms for removing viral aerosols of a submicrometer size, the overall viral aerosol filtration efficiency commonly decreases with the increase of face velocity. The pressure drop, however, is always positively correlated to the face velocity.

A number of theories and models have been developed to correlate the face velocity with the filtration efficiency and pressure drop.[96,97] However, the discussion about these theories is beyond the scope of this perspective and the readers are referred to these references.[55,96,97] Yeom et al. challenged a PA6/polyethylene (PE) bicomponent spunbond web with neutralized monodisperse DOP aerosols (0.015−0.4 μm) with face velocities ranging from 3.3 to 11.7 cm s^{-1}. The results confirmed the reduced aerosol filtration efficiency and increased pressure drop at higher face velocities. It is worth noting that the pressure drop linearly increased with the increase of the face velocity, which indicated a laminar air flow within the air filter.[98] Leung et al. deposited one layer of electrospun poly(ethylene oxide) (PEO) nanofibers with an average diameter of 208 nm onto the surface of a nonwoven microfiber air filter. Compared with the electrospun layer, the aerosol filtration efficiency and pressure drop of the substrate air filter were negligible. The composite filter was challenged by NaCl aerosols with a size ranging from 50 to 480 nm. The results indicated that for the whole aerosol size range the filtration efficiency decreased as the face velocity increased from 5 to 10 cm s^{-1}.[67] Interestingly, similar to the aerosol charge, the influence of the face velocity on the filtration efficiency for smaller aerosol particles, like 100 nm, was more significant than that on larger aerosols. Besides the lower diffusion collection efficiency, the increased face velocity also results in a reduced electrostatic collection efficiency. Sanchez et al. challenged the electrostatically charged fibrous filters with aerosols at face velocities of 50 to 250 cm s^{-1}. The reduced aerosol filtration efficiency at higher velocities was attributed to less time (shorter retention time) for electrostatic forces to take effect. The results also indicated that high face velocities (1.7 and 2.7 m s^{-1}) might induce aerosol particle bounce, which deteriorated the overall filtration efficiency, i.e., 10−15% reduction of the filtration efficiency when compared to that under a low face velocity (0.5 m s^{-1}).[86] Face velocity varies depending on different inhalation regimes. For example, Eninger et al. utilized viral aerosol airflows with three different flow rates, i.e., 30, 85, and 150 L min^{-1}, to challenge N99 and N95 respirators. Among three flow rates, 30 and 85 L min^{-1} represented the inhalation modes of a low/moderate and a hard workload, respectively, while 150 L min^{-1} mimicked the instantaneous peak inspiratory flow of the moderate/hard workload.[99] Therefore, a series of face velocities which could represent different breathing modes should be selected to test the aerosol filtration performance of electrospun membranes.

3.2.2. Temperature and Air Humidity. Generally speaking, the fluctuation of temperature during the filtration tests may not significantly affect the aerosol filtration efficiency and pressure drop, especially within the narrow temperature range in which face masks, respirators, and air filters perform. In contrast, air humidity is found to significantly influence the aerosol filtration performance, especially when the air humidity varies during the aerosol filtration process. However, how the filtration efficiency and pressure drop change with air humidity depends on the characteristics of aerosol particles (hygroscopicity and size) and filter media (hydrophilicity).

Montgomery et al. found that for the HVAC filters loaded with NaCl (hygroscopic), Al_2O_3 (nonhygroscopic), or a mixture of these two particles, the filtration efficiency and pressure drop responded differently to the change of RH. Specifically, both the filtration efficiency for removing 130 nm particles of NaCl and pressure drop of NaCl-loaded HVAC filters decreased with an elevation of RH. In contrast, HVAC filters loaded with Al_2O_3 showed a small decrease in the pressure drop and almost no change in the aerosol filtration efficiency at a higher RH.[100] Similarly, Gupta et al. and Miguel et al. reported a reduced pressure drop at relatively high RH (but lower than the deliquescent point of NaCl) for NaCl-loaded air filters in filtration.[101,102] However, Kim et al. concluded that the filtration efficiency of glass fibrous air filters for removing NaCl aerosols did not vary with respect to the air

https://doi.org/10.1021/acsenvironau.1c00047
ACS Environ. Au 2022, 2, 290−309

humidity. Their explanation was that the size of challenge aerosols was relatively small, i.e., <100 nm. It is worth noting that the glass fibrous air filters used in this study were not preloaded with aerosol particles, which may be another important reason for the unchanged filtration efficiency.[103] The aforementioned results indicate that with the accumulation of aerosol particles in the filtration media, the filtration performance may significantly change even at the same RH. Xu et al. investigated the change of vehicle cabin filters' performance after being exposed to humid air. The filtration efficiency and pressure drop were continuously monitored when air filters were operated at 5%, 62%, and 90% RH. With the passage of time, water absorption by dusts trapped within the air filters resulted in a significant increase of both the filtration efficiency (up to 15% for particles with a size of 0.3 to 5 μm) and pressure drop (up to 250 pa).[104] Wang et al. further took the hydrophobicity of the filter media into consideration. They first fabricated a series of air filters comprising fibers with different hydrophilicity, i.e., PVDF fiber (hydrophobic), PAN fiber (hydrophilic), and a dual layer of PAN/PVDF fiber. Next, three filters were challenged by NaCl and Al_2O_3 aerosols at 40% and 80% RH. Consistent with previous studies, all three unloaded (clean) air filters showed almost unchanged filtration efficiency against NaCl and Al_2O_3 aerosols at both RH of 80% and 40%. In addition, the evolution of filtration efficiency and pressure drop for continuous NaCl (12 h) and Al_2O_3 (24 h) aerosol exposure was monitored at both RHs. The results indicated a consistent aerosol filtration efficiency during the long-term filtration processes for both aerosols at both RHs. However, the increment pattern of pressure drop was only affected by the hygroscopicity of aerosol particles and hydrophilicity of filter media at a higher RH of 80%.[105] Currently, to avoid the complication of RH on filtration performance, most aerosol filtration studies utilize a dryer to remove the moisture of aerosols (Table 2), which does not always mimic real scenarios in engineering applications. For example, when intended for applications as face masks and respirators, electrospun nanofibrous membranes are expected to experience a higher RH compared with being used as indoor air filters.[106,107] Therefore, the air humidity in aerosol filtration tests should be adjusted according to diverse applications of electrospun nanofibrous membranes.

3.2.3. Membrane Installation and Leakage. To monitor the aerosol filtration performance, electrospun nanofibrous membranes are always installed in either customized or commercial filtration test systems. For most studies, the tested membranes are tightly accommodated by a filter holder, which completely avoids the leakage. This strategy is suitable for evaluating the performance of common air filters since no leakage is expected during their daily operation. However, for electrospun nanofibrous membranes intended for face masks, the tight membrane installation without considering mask fit only measures the optimum filtration efficiency and thus may always overestimate the protective effectiveness. Even though in tightly sealed systems the effects of a poor mask fit have been simulated by punching holes in tested membranes or connecting tubes, the filtration results are highly sensitive to the area and arrangement of the holes which are quite arbitrary in each study. For example, Konda et al. investigated the aerosol filtration performance of common fabrics which could be used for constructing face masks worn by the general public. For mimicking the improper fit of face masks, symmetrical holes with total opening area of 0.5−2% of the membrane area were drilled in the connecting tubes. The results indicated that the gaps caused by these holes resulted in more than a 60% decrease in the aerosol filtration efficiency.[108] Similarly, to investigate the influence of leakage on filtration performance, Drewnick et al. punched out three holes from one surgical mask and one velvet cotton sample. The total area of these holes was 0.5%, 1%, and 2% of the active membrane area in three separate filtration tests. The results indicated that even a small leak (1%) could lead to a huge reduction in the aerosol filtration efficiency (reduction by 50% for particle size less than 2.5 μm). However, even the authors admitted that the study was only a qualitative assessment of the effects of leakage on the face masks' performance and more delicate experiments would be needed in the future.[13] Therefore, to better understand the fit status, manikin or human based aerosol filtration test systems are recommended for the electrospun nanofibrous membranes intended for face mask applications. In a study, volunteers, including healthy subjects and simulated patients, were recruited to assess the inward protection of different types of face masks. In addition, an artificial test head on which face masks were mounted was utilized to evaluate the outward protection of the samples. It is found that the outward protection of all the face masks was lower than inward protection, which might be attributed to different amounts of leakage occurring during two modes.[109] By combining the manikin-based filtration test system and visualization of air leakage, Ortiz et al. investigated the outward leakage of different types of face masks. As expected, more leakage was observed from face masks with loose fit.[110] Similarly, Pan et al. investigated the filtration efficiency of different cloth masks, a surgical mask, and a face shield under ideal conditions (i.e., in a tight filter holder). In addition, inward and outward protection of all the samples was evaluated on a manikin. The results indicated that a reduced filtration efficiency was observed on the manikin compared with that in the tightly sealed filter holder due to the gaps in the manikin-based tests.[111] It is also worth noting that in manikin-based filtration test systems, the membrane samples could also be tightly attached on the dummy head by sealant to measure the maximum aerosol filtration efficiency of face masks. In conclusion, for electrospun membranes intended for diverse applications, different membrane installation methods should be employed. For example, if the electrospun membranes are intended for face mask applications, the manikin-based filtration test system should be utilized since mask fit is taken into consideration. For indoor air filters, however, electrospun membranes should be installed in a tight filter holder since little to no leakage is expected during the operation of these filters.

3.3. Aerosol Collection and Detection

For most studies using nonbiological surrogates for aerosol filtration tests, the amount and size distribution of aerosols upstream and downstream of the tested membranes are usually directly measured by various aerosol detection instruments based on the mass, the surface area, or the number *in situ*. The mechanisms and applications of these aerosol detection instruments have been thoroughly discussed by Wang et al.[55] Thereafter, the aerosol filtration efficiency (E) is calculated based on

$$E = 1 - C_{\text{downstream}}/C_{\text{upstream}} \quad (2)$$

https://doi.org/10.1021/acsenvironau.1c00047
ACS Environ. Au 2022, 2, 290−309

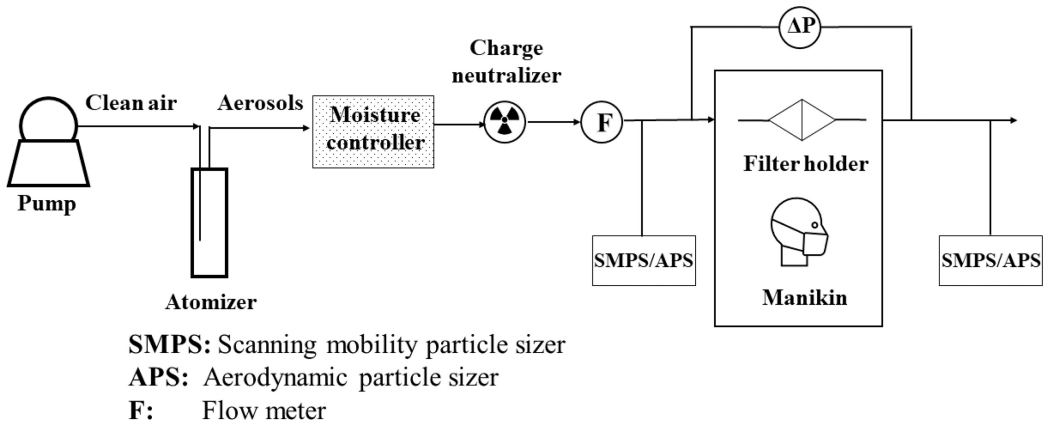

Figure 5. Schematic of standardized protocol for aerosol filtration tests.

in which $C_{downstream}$ and $C_{upstream}$ are aerosol concentrations before and after going through the tested membranes, respectively.

For viral aerosols, however, the viral load, including total and infectious load, instead of aerosol particle numbers is always of interest. To investigate the viral load, the viral aerosols in the filtration tests usually undergo a "collection and detection" process. The collection of viral aerosols can be achieved by filtration, impingement, impaction, and electrostatic precipitation.[112] However, it is worth noting that different sampling methods may lead to varying collection efficiency, and some methods could even fail to achieve satisfactory collection of the viral aerosols. For example, a series of studies have discussed the influence of various filter media on the collection efficiency of bioaerosols.[113,114] Verreault et al. utilized polycarbonate (PC) and polytetrafluoroethylene (PTFE) air filters to collect aerosolized bacteriophages ϕX174 and P008. Results from both quantitative polymerase chain reaction (qPCR) and plaque assays for quantifying the total and infectious viruses, respectively, indicated that the PC air filter performed better for viral aerosol collection.[75] Similarly, Gendron et al. investigated the performance of PTFE and PC filters for collecting aerosolized bacteriophages ϕ 6 and MS2. The results indicated that PC filters were superior for collecting infectious viruses (as indicated by plaque assays), but both PTFE and PC filters were equally efficient for collecting total virus regardless of infectivity (as determined by the reverse transcription-quantitative polymerase chain reaction (RT-qPCR)).[42] In contrast, Burton et al. evaluated the collection efficiency of PTFE, gelatin, and PC filters for MS2 virion particles with a diameter of 10−80 nm. Compared with PC filters, PTFE and gelatin filters showed a better collection efficiency. Specifically, both PTFE and gelatin filters possessed a filtration efficiency higher than 96%, while the optimal PC filter only had a filtration efficiency of 68%.[115] Given the discrepancy in the viral aerosol collection efficiency caused by different filter materials, the gelatin filter is recommended for collecting viral aerosols in aerosol filtration tests due to excellent performance.[76,115] In addition, the gelatin filter could be dissolved into water, which avoids the challenges associated with virus recovery from the filter for quantification and simplifies the determination of both total and infectious viral load.[116] Furthermore, Biswas et al. evaluated the collection efficiency of three different samplers, i.e., the All Glass Impinger 30 (AGI-30), the SKC BioSampler, and a frit bubbler for collecting bacteriophage MS2 and T3 aerosols. The results indicated that all the samplers had about 10% or even lower collection efficiency for collecting viral aerosols with a size ranging from 30 to 100 nm.[76] In terms of virus detection, just as what Verreault et al. did, qPCR and culture methods (e.g., plaque assays, median tissue culture infectious dose ($TCID_{50}$), and integrated cell culture-quantitative polymerase chain reaction (ICC-qPCR)) are generally used to determine the total and infectious viral load, respectively. However, the viral load in the air is low and the infectivity of airborne viruses is thus not always quantifiable. It is worth noting that sometimes only one bioaerosol sampler was installed downstream of tested filters. In this case, the aerosol filtration efficiency should be calculated as

$$E = 1 - C_{with}/C_{without} \quad (3)$$

where C_{with} and $C_{without}$ are the viral load collected by the bioaerosol sampler with and without filters installed, respectively.

3.4. Standardization of Aerosol Filtration Tests for Electrospun Nanofibrous Membranes

As reviewed, previous aerosol filtration tests varied in aerosol generation, filtration, collection, and detection, which may impede the comparison across different studies. Therefore, for better understanding of the aerosol filtration performance of electrospun nanofibrous membranes, the standardized filtration test method is urgently needed. Herein, we propose one standardized aerosol filtration test protocol (Figure 5) based on the aforementioned discussion. In the protocol, aerosols containing viruses of interest instead of surrogates are generated by an atomizer. If conditions are not permitted, e.g., severe biosafety concerns caused by aerosolized pathogenic viruses such as SARS-CoV-2, surrogates of bacteriophages and animal viruses are better candidates for aerosol generation in the filtration test. Compared with nonbiological surrogates, viral surrogates better mimic the behavior of pathogenic viruses in filtration due to a similar size, structure, and biological nature. In addition, viral aerosols with a wide range of particle sizes, i.e., from tens of nanometers to several micrometers, should be generated from liquids that best simulate biological fluids (e.g., simulated or real saliva). To eliminate the influence of the aerosol charge on the filtration performance, generated aerosols should pass through a neutralizer. After neutralization, the charge of aerosols follows the Boltzmann distribution but the net charge is zero. The size and concentration distributions of aerosols upstream and

https://doi.org/10.1021/acsenvironau.1c00047
ACS Environ. Au 2022, 2, 290−309

downstream of the test membranes are monitored by the instruments like APS and SMPS. During aerosol filtration tests, the face velocity, temperature, and air humidity should be carefully adjusted according to intended applications of tested electrospun membranes. For example, when used for indoor air filters, the RH of the air flow carrying viral aerosols should be maintained within 30−50%, while the RH should be higher (∼100%) when the electrospun membranes are used for face masks and respirators. In the protocol, the air humidity and face velocity are controlled by the moisture controller and the flow meter, respectively. Furthermore, for electrospun nanofibrous membranes intended for face mask applications, mask fit should be taken into consideration by using manikin- or human-based filtration test systems. In the end, it is worth noting that for nonbiological aerosol surrogates and real viral aerosols, different instruments and methods for aerosol collection and detection should be employed and compared. Particularly, the optimized approach for maximizing viral aerosol collection and viral infectivity quantification should be adopted.

4. FUTURE DEVELOPMENT OF ELECTROSPUN NANOFIBROUS MEMBRANES

Even though electrospun nanofibrous membranes have shown promising performance for highly efficient aerosol removal, their wide applications are still limited, due to serious air pollution from solvents, inferior mechanical properties of the membranes, single usage of the membranes that leads to plastic waste, and unwieldy equipment for manufacturing (Figure 6).

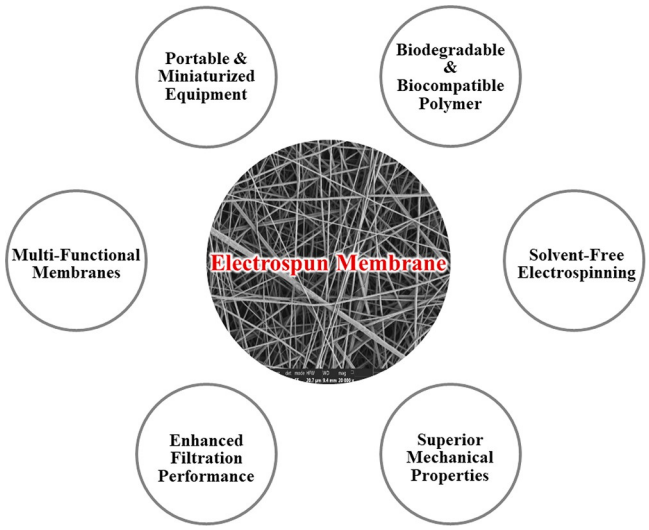

Figure 6. Future development of electrospun nanofibrous membranes for air filtration applications.

Advancements in the electrospinning technology are able to resolve the aforementioned issues. The upgraded electrospun nanofibrous membranes could be widely used in scenarios such as PPE and HVAC systems for efficiently removing airborne viruses. For example, electrospun nanofibrous membranes could be used to replace filter media within surgical masks, respirators, and indoor air filters. The viral aerosol filtration efficiency of homemade cloth masks could also be improved by incorporating electrospun nanofibrous membranes.

The pollution issue arises from both the electrospinning process and the disposal of electrospun products. Researchers already have concerns with semivolatile and volatile organic compounds emitted from the surgical masks.[117] So far, most research dissolved polymers in organic solvents for electrospinning. The organic solvents, like *N*,*N*-dimethyl formamide, evaporate and accumulate indoors during electrospinning, which is harmful to both the environment and human health.[118] In addition, residual solvents in the electrospun nanofibrous membranes may pose more health risks to the customers when the membranes are fabricated as face masks. Moreover, most polymeric materials used in electrospinning are non-biodegradable and unrecyclable. The piling up of waste electrospun products made from these plastic materials will pose a serious threat to the environment.[119] According to the concept of green electrospinning proposed by Lv et al., the pollution issue could be resolved by employing novel biodegradable polymers and green electrospinning techniques, e.g., water-based and solvent-free electrospinning.[24] Zhang et al. successfully electrospun biodegradable chitosan nanofibers *in situ* to achieve more than 95% removal of $PM_{2.5}$.[120] Similarly, Pakravan et al. synthesized biocompatible and biodegradable chitosan/PEO nanofibers with a diameter ranging from 60 to 80 nm by electrospinning both polymers in an acetic acid solution. Moreover, compared with trifluoroacetic acid which is well-established for chitosan electrospinning, acetic acid is more environmental friendly and nontoxic.[121] Furthermore, the water-based and solvent-free electrospinning techniques are able to avert the implementation of harmful organic solvents. Common water-soluble polymers which could be used for electrospinning include poly(acrylic acid) (PAA), PVA, PEO, polyvinylpyrrolidone (PVP), and hydroxypropyl cellulose. For example, Li et al. fabricated electrospun nanofibrous membranes from PVA and PAA in aqueous solutions. The fiber diameter could be tailored from 270 to 450 nm by adjusting the PAA content in the electrospinning dope solution.[122] However, it is worth noting that water-soluble polymers can dissolve if they are exposed to the humidity. Therefore, cross-linking is needed once the polymers are electrospun. Melt electrospinning, a typical example of solvent-free electrospinning, can synthesize ultrafine fibers from a wide variety of polymers, including the ones that are not soluble in any solvents.[123] Buivydiene et al. fabricated a series of air filters via melt electrospinning polyamide and polyolefin-based polymers. The product air filters were characterized for the average fiber diameter and challenged by PM_1 in aerosol filtration tests. The optimum air filter could remove up to 80% of PM_1 with a QF of 0.0133 Pa^{-1}.[124]

Membranes intended for air filtration applications are always expected to show adequate mechanical strength, which limits the wide application of electrospun nanofibrous membranes in this field. The poor mechanical strength of electrospun nanofibrous membranes is mainly attributed to their highly porous structure, weak interactions between fibers, and intrinsic fiber properties such as the diameter and modulus.[125,126] So far, intensive efforts have been conducted to improve the mechanical properties of electrospun nanofibrous membranes. Huang et al. chemically modified the electrospun PAN and polysulfone nanofibrous membranes using polydopamine. The chemical modification improved the interactions between nanofibers, which resulted in a 100−300% enhancement in the mechanical strength.[127] Similarly, for improving the bonding between electrospun nanofibers, Choi et al. thermally treated the electrospun PVDF mats at 150−160 °C

https://doi.org/10.1021/acsenvironau.1c00047
ACS Environ. Au 2022, 2, 290−309

to create the binding between fiber junctions. Compared with the untreated mats, the electrospun nanofibrous membranes treated at 160 °C for 2 h showed a 28.4%, 242%, and 15.1% increase in the modulus, tensile strength, and elongation at break, respectively.[128] Moreover, solvent vapor treatment by organic solvents, e.g., *N*,*N*-dimethyl formamide, can also improve the mechanical properties of electrospun nanofibrous membranes.[129] In addition, additives could be incorporated to improve the mechanical strength of a single nanofiber. Mack et al. utilized graphite nanoplatelets as reinforcements to enhance the thermal stability and mechanical strength of electrospun PAN nanofibers. It is worth noting that with the increase of graphite nanoplatelets incorporated into the electrospun nanofibers, the modulus also increased. Compared with the pristine electrospun fibers, the PAN fibers incorporated with 4 wt % of graphite nanoplatelets showed a 200% increase in the Young's modulus.[130] Another approach commonly used to improve the mechanical strength of electrospun nanofibrous membranes is to deposit the nanofibers onto a rigid substrate, e.g., nonwoven microfibrous media.[67] The supporting layer generally does not contribute to the aerosol removal and pressure drop.

Besides environmental friendliness and mechanical strength, future research should focus on imparting more desirable properties to electrospun membranes. As reviewed in the section 2.3, multifunctional electrospun nanofibrous membranes, e.g., antimicrobial and microstrutured electrospun membranes, could be fabricated by incorporating functional nanoparticles into electrospinning.[131] For example, Chen et al. fabricated a super hydrophobic membrane by electrospinning, hydrothermal synthesis, and dip coating. ZnO nanowires were grown on the electrospun PVDF membrane via hydrothermal synthesis, from ZnO nanoparticles preloaded on the membrane. After dip-coating with oleic acid, the flexible composite membrane showed super hydrophobicity (with a water contact angle >150°) and excellent air permeability.[132] Wang et al. developed an electret polyethersulfone/barium titanate (PES/$BaTiO_3$) nanofibrous membrane by electrospinning a PES solution containing $BaTiO_3$ nanoparticles. The optimal nanofibrous membrane showed a filtration efficiency of 99.99% against $PM_{2.5}$ with a pressure drop of 67 Pa. Furthermore, the composite electrospun nanofibrous membranes possessed excellent wearing comfortability due to effective radiative cooling.[133] In addition, Li et al. synthesized photocatalytic self-cleaning masks by depositing nitrogen-doped TiO_2 onto membranes electrospun from a mixture of PVA, PEO, and cellulose nanofibers. These biodegradable electrospun membranes not only effectively inactivated bacteria under the irradiation of sunlight but also exhibited superior mechanical properties compared with a commercial single-use mask.[134] Zhang et al. fabricated nanofibrous mats overlaid by nanonets based on an electrospraying-netting technique. The hollow nanonets comprising nanowires (~12 nm) possessed a much smaller pore size than that formed between nanofibers (200−300 nm versus several micrometers). Therefore, a very high aerosol removal efficiency for $PM_{0.3}$ (>99.995%) and a low pressure drop (<91.2 Pa) were achieved.[135] Furthermore, when developed from piezoelectric materials (e.g., PVDF)[135] or triboelectric materials (e.g., a pair of materials that are more separated in the triboelectric series),[136] electrospun membranes can constantly translate mechanical vibration in airflow to charge, which enhances the electrostatic attraction for virus removal. Moreover, the attachment of molecular recognition elements such as antibodies, peptides, and polyvalent polymers enables electrospun nanofibrous membranes to selectively bind and capture pathogenic viruses of interest.[137] Last but not least, miniaturized and portable electrospinning apparatuses should be developed to simplify the electrospinning process. For large-scale industrial manufacturing, electrospinning apparatuses are always bulky and sometimes inconvenient. For example, Xu et al. pointed out that the conventional electrospinning setup is heavily dependent on the electricity supply, which restricts the production of electrospun membranes during power failure or in remote areas without a sustainable electricity supply.[19] In contrast, miniaturized and portable electrospinning apparatuses are promising alternatives to large-scale industrial manufacturing, especially for producing electrospun membranes with specific requirements for individuals and small communities.[19] Moreover, miniaturized and portable electrospinning can also generate membranes with highly tailored structures and properties easily, with a shorter startup time, when compared to industrial-scale electrospinning. In addition, the cost of transportation and distribution of electrospun nanofibrous membranes from factories to consumers may also be higher than those fabricated locally.

5. CONCLUSION

Electrospun nanofibrous membranes have emerged as promising candidates for controlling airborne viral pathogens, and they can thus find broad applications for PPE and indoor air filtration. These electrospun membranes have a reduced pore size, an increased porosity, and retained charges, and they have shown excellent performance for capturing virus-laden aerosols while maintaining a low pressure drop. However, the lack of a unified protocol impedes the comparison of electrospun membranes' filtration performance among different studies. In this perspective, we propose a standardized procedure for aerosol filtration testing, in which aerosol generation, filtration, collection, and detection are thoroughly considered. Particularly, aerosols generated from (simulated) biological fluids containing nonpathogenic viruses, instead of nonbiological surrogates like NaCl or PSL, should be used because they could best simulate the behavior of viral aerosols of interest in air filtration. Moreover, neutralized aerosols with a wide range of particle size, i.e., from tens of nanometers to several micrometers, are preferred. The face velocity, temperature, air humidity, and fit in the filtration test should be tailored depending on specific membrane applications for PPE or indoor air filtration. In addition, the optimized approach for maximizing the collection and quantification of viral aerosols should be adopted. Beyond standardizing the filtration test protocol, future work should also focus on advancing electrospinning by improving the filtration performance, antimicrobial capacity, and mechanical strength of the membrane, promoting an environmentally benign and sustainable manufacturing process, and adopting diverse manufacturing scales for personal, community, and industrial applications.

AUTHOR INFORMATION

Corresponding Authors

Hongchen Shen − *Department of Civil and Environmental Engineering, The George Washington University, Washington, DC 20052, United States*; Email: hongchenshen@gwu.edu

https://doi.org/10.1021/acsenvironau.1c00047
ACS Environ. Au 2022, 2, 290−309

Danmeng Shuai − *Department of Civil and Environmental Engineering, The George Washington University, Washington, DC 20052, United States;* orcid.org/0000-0003-3817-4092; Email: danmengshuai@gwu.edu

Authors

Minghao Han − *Department of Chemical and Environmental Engineering, University of California, Riverside, Riverside, California 92521, United States*

Yun Shen − *Department of Chemical and Environmental Engineering, University of California, Riverside, Riverside, California 92521, United States;* orcid.org/0000-0002-8225-1940

Complete contact information is available at: https://pubs.acs.org/10.1021/acsenvironau.1c00047

Notes

The authors declare no competing financial interest.

■ ACKNOWLEDGMENTS

We acknowledge the NSF RAPID grants (CBET-2029411 and CBET-2029330) for supporting our research.

■ REFERENCES

(1) Li, R.; Chen, B.; Zhang, T.; Ren, Z.; Song, Y.; Xiao, Y.; Hou, L.; Cai, J.; Xu, B.; Li, M.; Chan, K. K. Y.; Tu, Y.; Yang, M.; Yang, J.; Liu, Z.; Shen, C.; Wang, C.; Xu, L.; Liu, Q.; Bao, S.; Zhang, J.; Bi, Y.; Bai, Y.; Deng, K.; Zhang, W.; Huang, W.; Whittington, J. D.; Stenseth, N. C.; Guan, D.; Gong, P.; Xu, B. Global COVID-19 Pandemic Demands Joint Interventions for the Suppression of Future Waves. *Proc. Natl. Acad. Sci. U.S.A* **2020**, *117* (42), 26151−26157.

(2) CDC, Coronavirus disease 2019 (COVID-19); https://www.cdc.gov/coronavirus/2019-ncov/science/science-briefs/sars-cov-2-transmission.html, accessed: 05, 2021.

(3) WHO, Transmission of SARS-CoV-2: implications for infection prevention precautions: scientific brief; https://apps.who.int/iris/handle/10665/333114, accessed: 07, 2020.

(4) Jimenez, J.; Marr, L.; Randall, K.; Ewing, E. T.; Tufekci, Z.; Greenhalgh, T.; Milton, D. K.; Tellier, R.; Tang, J.; Li, Y.; Morawska, L.; Mesiano-Crookston, J.; Fisman, D.; Hegarty, O.; Dancer, S.; Bluyssen, P.; Buonanno, G.; Loomans, M.; Bahnfleth, W.; Yao, M.; Sekhar, C.; Wargocki, P.; Melikov, A. K.; Prather, K. *Echoes Through Time: The Historical Origins of the Droplet Dogma and Its Role in the Misidentification of Airborne Respiratory Infection Transmission*; SSRN Scholarly Paper ID 3904176; Social Science Research Network: Rochester, NY, 2021.

(5) Liu, Y.; Ning, Z.; Chen, Y.; Guo, M.; Liu, Y.; Gali, N. K.; Sun, L.; Duan, Y.; Cai, J.; Westerdahl, D.; Liu, X.; Xu, K.; Ho, K.; Kan, H.; Fu, Q.; Lan, K. Aerodynamic Analysis of SARS-CoV-2 in Two Wuhan Hospitals. *Nature* **2020**, *582* (7813), 557−560.

(6) Van Doremalen, N.; Bushmaker, T.; Morris, D. H.; Holbrook, M. G.; Gamble, A.; Williamson, B. N.; Tamin, A.; Harcourt, J. L.; Thornburg, N. J.; Gerber, S. I. Aerosol and Surface Stability of SARS-CoV-2 as Compared with SARS-CoV-1. *N. Engl. J. Med.* **2020**, *382* (16), 1564−1567.

(7) Wang, C. C.; Prather, K. A.; Sznitman, J.; Jimenez, J. L.; Lakdawala, S. S.; Tufekci, Z.; Marr, L. C. Airborne Transmission of Respiratory Viruses. *Science* **2021**, *373* (6558), No. eabd9149.

(8) Borro, L.; Mazzei, L.; Raponi, M.; Piscitelli, P.; Miani, A.; Secinaro, A. The Role of Air Conditioning in the Diffusion of Sars-CoV-2 in Indoor Environments: A First Computational Fluid Dynamic Model, Based on Investigations Performed at the Vatican State Children's Hospital. *Environ. Res.* **2021**, *193*, 110343.

(9) Stockman, T.; Zhu, S.; Kumar, A.; Wang, L.; Patel, S.; Weaver, J.; Spede, M.; Milton, D. K.; Hertzberg, J.; Toohey, D.; Vance, M.; Srebric, J.; Miller, S. L. Measurements and Simulations of Aerosol Released While Singing and Playing Wind Instruments. *ACS Environ. Au* **2021**, *1* (1), 71−84.

(10) Rowan, N. J.; Moral, R. A. Disposable Face Masks and Reusable Face Coverings as Non-Pharmaceutical Interventions (NPIs) to Prevent Transmission of SARS-CoV-2 Variants That Cause Coronavirus Disease (COVID-19): Role of New Sustainable NPI Design Innovations and Predictive Mathematical Modelling. *Science of The Total Environment* **2021**, *772*, 145530.

(11) Forouzandeh, P.; O'Dowd, K.; Pillai, S. C. Face Masks and Respirators in the Fight against the COVID-19 Pandemic: An Overview of the Standards and Testing Methods. *Saf. Sci.* **2021**, *133*, 104995.

(12) MacIntyre, C. R.; Dung, C. T.; Seale, H. S. Covid-19: Should Cloth Masks Be Used by Healthcare Workers as A Last Resort? *BMJ.* **2020**, *20* (15), 43.

(13) Drewnick, F.; Pikmann, J.; Fachinger, F.; Moormann, L.; Sprang, F.; Borrmann, S. Aerosol Filtration Efficiency of Household Materials for Homemade Face Masks: Influence of Material Properties, Particle Size, Particle Electrical Charge, Face Velocity, and Leaks. *Aerosol Sci. Technol.* **2021**, *55* (1), 63−79.

(14) Stephens, B.; Siegel, J. A. Ultrafine Particle Removal by Residential Heating, Ventilating, and Air-Conditioning Filters. *Indoor Air* **2013**, *23* (6), 488−497.

(15) Das, O.; Neisiany, R. E.; Capezza, A. J.; Hedenqvist, M. S.; Försth, M.; Xu, Q.; Jiang, L.; Ji, D.; Ramakrishna, S. The Need for Fully Bio-Based Facemasks to Counter Coronavirus Outbreaks: A Perspective. *Sci. Total Environ.* **2020**, *736*, 139611.

(16) Leung, W. W. F.; Sun, Q. Electrostatic Charged Nanofiber Filter for Filtering Airborne Novel Coronavirus (COVID-19) and Nano-Aerosols. *Sep. Purif. Technol.* **2020**, *250*, 116886.

(17) Choi, J.; Yang, B. J.; Bae, G.-N.; Jung, J. H. Herbal Extract Incorporated Nanofiber Fabricated by An Electrospinning Technique and Its Application to Antimicrobial Air Filtration. *ACS Appl. Mater. Interfaces* **2015**, *7* (45), 25313−25320.

(18) Matulevicius, J.; Kliucininkas, L.; Prasauskas, T.; Buivydiene, D.; Martuzevicius, D. The Comparative Study of Aerosol Filtration by Electrospun Polyamide, Polyvinyl Acetate, Polyacrylonitrile and Cellulose Acetate Nanofiber Media. *J. Aerosol Sci.* **2016**, *92*, 27−37.

(19) Xu, S.-C.; Qin, C.-C.; Yu, M.; Dong, R.-H.; Yan, X.; Zhao, H.; Han, W.-P.; Zhang, H.-D.; Long, Y.-Z. A Battery-Operated Portable Handheld Electrospinning Apparatus. *Nanoscale* **2015**, *7* (29), 12351−12355.

(20) Kai, D.; Liow, S. S.; Loh, X. J. Biodegradable Polymers for Electrospinning: Towards Biomedical Applications. *Mater. Sci. Eng., C* **2014**, *45*, 659−670.

(21) Blosi, M.; Costa, A. L.; Ortelli, S.; Belosi, F.; Ravegnani, F.; Varesano, A.; Tonetti, C.; Zanoni, I.; Vineis, C. Polyvinyl Alcohol/Silver Electrospun Nanofibers: Biocidal Filter Media Capturing Virus-Size Particles. *J. Appl. Polym. Sci.* **2021**, *138* (46), 51380.

(22) Selvam, A. K.; Nallathambi, G. Polyacrylonitrile/Silver Nanoparticle Electrospun Nanocomposite Matrix for Bacterial Filtration. *Fibers Polym.* **2015**, *16* (6), 1327−1335.

(23) Shen, H.; Zhou, Z.; Wang, H.; Zhang, M.; Han, M.; Durkin, D. P.; Shuai, D.; Shen, Y. Development of Electrospun Nanofibrous Filters for Controlling Coronavirus Aerosols. *Environ. Sci. Technol. Lett.* **2021**, *8* (7), 545−550.

(24) Lv, D.; Zhu, M.; Jiang, Z.; Jiang, S.; Zhang, Q.; Xiong, R.; Huang, C. Green Electrospun Nanofibers and Their Application in Air Filtration. *Macromol. Mater. Eng.* **2018**, *303* (12), 1800336.

(25) Sundarrajan, S.; Tan, K. L.; Lim, S. H.; Ramakrishna, S. Electrospun Nanofibers for Air Filtration Applications. *Procedia Eng.* **2014**, *75*, 159−163.

(26) Zhu, M.; Han, J.; Wang, F.; Shao, W.; Xiong, R.; Zhang, Q.; Pan, H.; Yang, Y.; Samal, S. K.; Zhang, F.; Huang, C. Electrospun Nanofibers Membranes for Effective Air Filtration. *Macromol. Mater. Eng.* **2017**, *302* (1), 1600353.

(27) Lyu, C.; Zhao, P.; Xie, J.; Dong, S.; Liu, J.; Rao, C.; Fu, J. Electrospinning of Nanofibrous Membrane and Its Applications in Air Filtration: A Review. *Nanomaterials* **2021**, *11* (6), 1501.

(28) Deng, Y.; Lu, T.; Cui, J.; Keshari Samal, S.; Xiong, R.; Huang, C. Bio-Based Electrospun Nanofiber as Building Blocks for a Novel Eco-Friendly Air Filtration Membrane: A Review. *Sep. Purif. Technol.* **2021**, *277*, 119623.
(29) Yang, W.; Elankumaran, S.; Marr, L. C. Concentrations and Size Distributions of Airborne Influenza A Viruses Measured Indoors at A Health Centre, A Day-Care Centre and on Aeroplanes. *J. R. Soc. Interface* **2011**, *8* (61), 1176−1184.
(30) Office of the Federal Register, *N. A. and R. A. 21 CFR 878.4040 - Surgical apparel*; https://www.govinfo.gov/app/details/CFR-2004-title21-vol8/CFR-2004-title21-vol8-sec878-4040/https%3A%2F%2Fwww.govinfo.gov%2Fapp%2Fdetails%2FCFR-2004-title21-vol8%2FCFR-2004-title21-vol8-sec878-4040%2Fsummary, 2021.
(31) FDA, N95 Respirators, Surgical Masks, Face Masks, and Barrier Face Coverings, https://www.fda.gov/medical-devices/personal-protective-equipment-infection-control/n95-respirators-surgical-masks-face-masks-and-barrier-face-coverings, 2021.
(32) CDC, *42 CFR Part 84 Respiratory Protective Devices*; https://www.cdc.gov/niosh/npptl/topics/respirators/pt84abs2.html, 2021.
(33) Martin, S. B.; Moyer, E. S. Electrostatic Respirator Filter Media: Filter Efficiency and Most Penetrating Particle Size Effects. *J. Occup. Environ. Hyg.* **2000**, *15* (8), 609−617.
(34) Tcharkhtchi, A.; Abbasnezhad, N.; Zarbini Seydani, M.; Zirak, N.; Farzaneh, S.; Shirinbayan, M. An Overview of Filtration Efficiency through the Masks: Mechanisms of the Aerosols Penetration. *Bioact. Mater.* **2021**, *6* (1), 106−122.
(35) Makison Booth, C.; Clayton, M.; Crook, B.; Gawn, J. M. Effectiveness of Surgical Masks against Influenza Bioaerosols. *J. Hosp. Infect.* **2013**, *84* (1), 22−26.
(36) Bałazy, A.; Toivola, M.; Reponen, T.; Podgórski, A.; Zimmer, A.; Grinshpun, S. A. Manikin-Based Performance Evaluation of N95 Filtering-Facepiece Respirators Challenged with Nanoparticles. *Ann. Occup. Hyg.* **2006**, *50* (3), 259−269.
(37) Bałazy, A.; Toivola, M.; Adhikari, A.; Sivasubramani, S. K.; Reponen, T.; Grinshpun, S. A. Do N95 Respirators Provide 95% Protection Level against Airborne Viruses, and How Adequate Are Surgical Masks? *Am. J. Infect. Control* **2006**, *34* (2), 51−57.
(38) Lee, S.-A.; Grinshpun, S. A.; Reponen, T. Respiratory Performance Offered by N95 Respirators and Surgical Masks: Human Subject Evaluation with NaCl Aerosol Representing Bacterial and Viral Particle Size Range. *Ann. Occup. Hyg.* **2008**, *52* (3), 177−185.
(39) Wen, Z.; Yu, L.; Yang, W.; Hu, L.; Li, N.; Wang, J.; Li, J.; Lu, J.; Dong, X.; Yin, Z.; Zhang, K. Assessment the Protection Performance of Different Level Personal Respiratory Protection Masks against Viral Aerosol. *Aerobiologia* **2013**, *29* (3), 365−372.
(40) Zangmeister, C. D.; Radney, J. G.; Vicenzi, E. P.; Weaver, J. L. Filtration Efficiencies of Nanoscale Aerosol by Cloth Mask Materials Used to Slow the Spread of SARS-CoV-2. *ACS Nano* **2020**, *14* (7), 9188−9200.
(41) Rengasamy, S.; Eimer, B.; Shaffer, R. E. Simple Respiratory Protection—Evaluation of the Filtration Performance of Cloth Masks and Common Fabric Materials Against 20−1000 nm Size Particles. *Ann. Occup. Hyg.* **2010**, *54* (7), 789−798.
(42) Gendron, L.; Verreault, D.; Veillette, M.; Moineau, S.; Duchaine, C. Evaluation of Filters for the Sampling and Quantification of RNA Phage Aerosols. *Aerosol Sci. Technol.* **2010**, *44* (10), 893−901.
(43) Davies, A.; Thompson, K.-A.; Giri, K.; Kafatos, G.; Walker, J.; Bennett, A. Testing the Efficacy of Homemade Masks: Would They Protect in An Influenza Pandemic? *Disaster Med. Public Health Prep.* **2013**, *7* (4), 413−418.
(44) Sharma, S. K.; Mishra, M.; Mudgal, S. K. Efficacy of Cloth Face Mask in Prevention of Novel Coronavirus Infection Transmission: A Systematic Review and Meta-Analysis. *J. Edu.c Health Promot.* **2020**, *9*, 192.
(45) Shakya, K. M.; Noyes, A.; Kallin, R.; Peltier, R. E. Evaluating the Efficacy of Cloth Facemasks in Reducing Particulate Matter Exposure. *J. Expo. Sci. Environ. Epidemiol.* **2017**, *27* (3), 352−357.
(46) ASHRAE, ANSI/ASHRAE Standard 52.2−2017. 62. https://www.ashrae.org/File%20Library/Technical%20Resources/COVID-19/52_2_2017_COVID-19_20200401.pdf.
(47) Huang, R.; Agranovski, I.; Pyankov, O.; Grinshpun, S. Removal of Viable Bioaerosol Particles with A Low-Efficiency HVAC Filter Enhanced by Continuous Emission of Unipolar Air Ions. *Indoor Air* **2008**, *18* (2), 106−112.
(48) Hyun, J.; Lee, S.-G.; Hwang, J. Application of Corona Discharge-Generated Air Ions for Filtration of Aerosolized Virus and Inactivation of Filtered Virus. *J. Aerosol Sci.* **2017**, *107*, 31−40.
(49) Park, K.-T.; Hwang, J. Filtration and Inactivation of Aerosolized Bacteriophage MS2 by A CNT Air Filter Fabricated Using Electro-Aerodynamic Deposition. *Carbon* **2014**, *75*, 401−410.
(50) Zhang, J.; Huntley, D.; Fox, A.; Gerhardt, B.; Vatine, A.; Cherne, J. Study of Viral Filtration Performance of Residential HVAC Filters. *ASHRAE J.* **2020**, *62* (8), 26−32.
(51) Novick, V. J.; Monson, P. R.; Ellison, P. E. The Effect of Solid Particle Mass Loading on the Pressure Drop of HEPA Filters. *J. Aerosol Sci.* **1992**, *23* (6), 657−665.
(52) Helmbuch, B. K.; Hodge, J. K.; Wander, J. D. *Viral Penetration of High Efficiency Particulate Air (HEPA) Filters*; Applied Research Associates Inc.: Tyndall AFB FL, 2007.
(53) Lu, T.; Cui, J.; Qu, Q.; Wang, Y.; Zhang, J.; Xiong, R.; Ma, W.; Huang, C. Multistructured Electrospun Nanofibers for Air Filtration: A Review. *ACS Appl. Mater. Interfaces* **2021**, *13* (20), 23293−23313.
(54) Dunnett, S. Filtration Mechanisms. In *Aerosol Science*; John Wiley & Sons, Ltd, 2013; pp 89−117.
(55) Wang, J.; Tronville, P. Toward Standardized Test Methods to Determine the Effectiveness of Filtration Media against Airborne Nanoparticles. *J. Nanopart. Res.* **2014**, *16* (6), 2417.
(56) Chattopadhyay, S.; Hatton, T. A.; Rutledge, G. C. Aerosol Filtration Using Electrospun Cellulose Acetate Fibers. *J. Mater. Sci.* **2016**, *51* (1), 204−217.
(57) Zhao, X.; Wang, S.; Yin, X.; Yu, J.; Ding, B. Slip-Effect Functional Air Filter for Efficient Purification of $PM_{2.5}$. *Sci. Rep.* **2016**, *6* (1), 35472.
(58) Zhang, Q.; Welch, J.; Park, H.; Wu, C.-Y.; Sigmund, W.; Marijnissen, J. C. M. Improvement in Nanofiber Filtration by Multiple Thin Layers of Nanofiber Mats. *J. Aerosol Sci.* **2010**, *41* (2), 230−236.
(59) Balgis, R.; Kartikowati, C. W.; Ogi, T.; Gradon, L.; Bao, L.; Seki, K.; Okuyama, K. Synthesis and Evaluation of Straight and Bead-Free Nanofibers for Improved Aerosol Filtration. *Chem. Eng. Sci.* **2015**, *137*, 947−954.
(60) Hung, C.-H.; Leung, W. W.-F. Filtration of Nano-Aerosol Using Nanofiber Filter under Low Peclet Number and Transitional Flow Regime. *Sep. Purif. Technol.* **2011**, *79* (1), 34−42.
(61) Park, K.; Kang, S.; Park, J.; Hwang, J. Fabrication of Silver Nanowire Coated Fibrous Air Filter Medium via A Two-Step Process of Electrospinning and Electrospray for Anti-Bioaerosol Treatment. *J. Hazard. Mater.* **2021**, *411*, 125043.
(62) Al-Attabi, R.; Morsi, Y.; Kujawski, W.; Kong, L.; Schütz, J. A.; Dumée, L. F. Wrinkled Silica Doped Electrospun Nano-Fiber Membranes with Engineered Roughness for Advanced Aerosol Air Filtration. *Sep. Purif. Technol.* **2019**, *215*, 500−507.
(63) Wang, N.; Si, Y.; Wang, N.; Sun, G.; El-Newehy, M.; Al-Deyab, S. S.; Ding, B. Multilevel Structured Polyacrylonitrile/Silica Nanofibrous Membranes for High-Performance Air Filtration. *Sep. Purif. Technol.* **2014**, *126*, 44−51.
(64) Shen, H.; Zhou, Z.; Wang, H.; Chen, J.; Zhang, M.; Han, M.; Shen, Y.; Shuai, D. Photosensitized Electrospun Nanofibrous Filters for Capturing and Killing Airborne Coronaviruses under Visible Light Irradiation. *Environ. Sci. Technol.* **2022**, DOI: 10.1021/acs.est.2c00885.
(65) Liu, Y.; Park, M.; Ding, B.; Kim, J.; El-Newehy, M.; Al-Deyab, S. S.; Kim, H.-Y. Facile Electrospun Polyacrylonitrile/Poly(Acrylic

Acid) Nanofibrous Membranes for High Efficiency Particulate Air Filtration. *Fibers Polym.* **2015**, *16* (3), 629−633.
(66) Song, J.; Zhao, Q.; Meng, C.; Meng, J.; Chen, Z.; Li, J. Hierarchical Porous Recycled PET Nanofibers for High-Efficiency Aerosols and Virus Capturing. *ACS Appl. Mater. Interfaces* **2021**, *13* (41), 49380−49389.
(67) Leung, W. W.-F.; Hung, C.-H.; Yuen, P.-T. Effect of Face Velocity, Nanofiber Packing Density and Thickness on Filtration Performance of Filters with Nanofibers Coated on A Substrate. *Sep. Purif. Technol.* **2010**, *71* (1), 30−37.
(68) de Almeida, D. S.; Martins, L. D.; Muniz, E. C.; Rudke, A. P.; Squizzato, R.; Beal, A.; de Souza, P. R.; Bonfim, D. P. F.; Aguiar, M. L.; Gimenes, M. L. Biodegradable CA/CPB Electrospun Nanofibers for Efficient Retention of Airborne Nanoparticles. *Process Saf. Environ. Prot.* **2020**, *144*, 177−185.
(69) Liu, J.; Qi, R.; Li, Q.; Han, G.; Qi, J. Filtration of Bioaerosols Using Fibrous Air Filter Media. *HVAC&R Res.* **2009**, *15* (6), 1165−1174.
(70) Miaskiewicz-Peska, E.; Lebkowska, M. Comparison of Aerosol and Bioaerosol Collection on Air Filters. *Aerobiologia* **2012**, *28* (2), 185−193.
(71) Gorny, R.; Dutkiewicz, J.; Krysinska-Traczyk, E. Size Distribution of Bacterial and Fungal Bioaerosols in Indoor Air. *Ann. Agric. Environ. Med.* **1999**, *6*, 105−113.
(72) Trunov, M.; Trakumas, S.; Willeke, K.; Grinshpun, S. A.; Reponen, T. Collection of Bioaerosol Particles by Impaction: Effect of Fungal Spore Agglomeration and Bounce. *Aerosol Sci. Technol.* **2001**, *35* (1), 617−624.
(73) Pan, M.; Carol, L.; Lednicky, J. A.; Eiguren-Fernandez, A.; Hering, S.; Fan, Z. H.; Wu, C.-Y. Determination of the Distribution of Infectious Viruses in Aerosol Particles Using Water-Based Condensational Growth Technology and A Bacteriophage MS2Model. *Aerosol Sci. Technol.* **2019**, *53* (5), 583−593.
(74) Yu, L.; Wen, Z.; Li, J.; Yang, W.; Wang, J.; Li, N.; Lu, J. Effects of Different Sampling Solutions on the Survival of Bacteriophages in Bubbling Aeration. *Aerobiologia* **2010**, *26* (1), 75−82.
(75) Verreault, D.; Rousseau, G. M.; Gendron, L.; Massé, D.; Moineau, S.; Duchaine, C. Comparison of Polycarbonate and Polytetrafluoroethylene Filters for Sampling of Airborne Bacteriophages. *Aerosol Sci. Technol.* **2010**, *44* (3), 197−201.
(76) Hogan, C. j., Jr; Kettleson, E. m.; Lee, M.-H.; Ramaswami, B.; Angenent, L. t.; Biswas, P. Sampling Methodologies and Dosage Assessment Techniques for Submicrometre and Ultrafine Virus Aerosol Particles. *J. Appl. Microbiol.* **2005**, *99* (6), 1422−1434.
(77) Lute, S.; Aranha, H.; Tremblay, D.; Liang, D.; Ackermann, H. W.; Chu, B.; Moineau, S.; Brorson, K. Characterization of Coliphage PR772 and Evaluation of Its Use for Virus Filter Performance Testing. *Appl. Environ. Microbiol.* **2004**, *70* (8), 4864−71.
(78) Turgeon, N.; Toulouse, M.-J.; Martel, B.; Moineau, S.; Duchaine, C. Comparison of Five Bacteriophages as Models for Viral Aerosol Studies. *Appl. Environ. Microbiol.* **2014**, *80* (14), 4242−4250.
(79) Zuo, Z.; Kuehn, T. H.; Verma, H.; Kumar, S.; Goyal, S. M.; Appert, J.; Raynor, P. C.; Ge, S.; Pui, D. Y. H. Association of Airborne Virus Infectivity and Survivability with Its Carrier Particle Size. *Aerosol Sci. Technol.* **2013**, *47* (4), 373−382.
(80) Zuo, Z.; Kuehn, T. H.; Bekele, A. Z.; Mor, S. K.; Verma, H.; Goyal, S. M.; Raynor, P. C.; Pui, D. Y. H. Survival of Airborne MS2 Bacteriophage Generated from Human Saliva, Artificial Saliva, and Cell Culture Medium. *Appl. Environ. Microbiol.* **2014**, *80* (9), 2796−2803.
(81) Smither, S. J.; Eastaugh, L. S.; Findlay, J. S.; Lever, M. S. Experimental Aerosol Survival of SARS-CoV-2 in Artificial Saliva and Tissue Culture Media at Medium and High Humidity. *Emerg. Microbes Infect.* **2020**, *9* (1), 1415−1417.
(82) Stiti, M.; Castanet, G.; Corber, A.; Alden, M.; Berrocal, E. Transition from Saliva Droplets to Solid Aerosols in the Context of COVID-19 Spreading. *Environ. Res.* **2022**, *204*, 112072.
(83) Woo, M.-H.; Grippin, A.; Anwar, D.; Smith, T.; Wu, C.-Y.; Wander, J. D. Effects of Relative Humidity and Spraying Medium on UV Decontamination of Filters Loaded with Viral Aerosols. *Appl. Environ. Microbiol.* **2012**, *78* (16), 5781−5787.
(84) Johnson, G. R.; Morawska, L.; Ristovski, Z. D.; Hargreaves, M.; Mengersen, K.; Chao, C. Y. H.; Wan, M. P.; Li, Y.; Xie, X.; Katoshevski, D.; Corbett, S. Modality of Human Expired Aerosol Size Distributions. *J. Aerosol Sci.* **2011**, *42* (12), 839−851.
(85) Yan, J.; Grantham, M.; Pantelic, J.; Mesquita, P. J. B. de; Albert, B.; Liu, F.; Ehrman, S.; Milton, D. K.; Consortium, E. Infectious Virus in Exhaled Breath of Symptomatic Seasonal Influenza Cases from A College Community. *Proc. Natl. Acad. Sci. U.S.A* **2018**, *115* (5), 1081−1086.
(86) Sanchez, A. L.; Hubbard, J. A.; Dellinger, J. G.; Servantes, B. L. Experimental Study of Electrostatic Aerosol Filtration at Moderate Filter Face Velocity. *Aerosol Sci. Technol.* **2013**, *47* (6), 606−615.
(87) Ruzer, L. S.; Harley, N. H. *Aerosols Handbook: Measurement, Dosimetry, and Health Effects*, 2nd ed.; CRC Press, 2012.
(88) Khlystov, A.; Stanier, C.; Pandis, S. N. An Algorithm for Combining Electrical Mobility and Aerodynamic Size Distributions Data When Measuring Ambient Aerosol Special Issue of Aerosol Science and Technology on Findings from the Fine Particulate Matter Supersites Program. *Aerosol Sci. Technol.* **2004**, *38* (sup1), 229−238.
(89) Mainelis, G.; Willeke, K.; Baron, P.; Grinshpun, S. A.; Reponen, T. Induction Charging and Electrostatic Classification of Micrometer-Size Particles for Investigating the Electrobiological Properties of Airborne Microorganisms. *Aerosol Sci. Technol.* **2002**, *36* (4), 479−491.
(90) Hogan, C. J.; Lee, M.-H.; Biswas, P. Capture of Viral Particles in Soft X-Ray-Enhanced Corona Systems: Charge Distribution and Transport Characteristics. *Aerosol Sci. Technol.* **2004**, *38* (5), 475−486.
(91) Duarte Fo, O. B.; Marra, W. D.; Kachan, G. C.; Coury, J. R. Filtration of Electrified Solid Particles. *Ind. Eng. Chem. Res.* **2000**, *39* (10), 3884−3895.
(92) Kim, M.; Zydney, A. L. Effect of Electrostatic, Hydrodynamic, and Brownian Forces on Particle Trajectories and Sieving in Normal Flow Filtration. *J. Colloid Interface Sci.* **2004**, *269* (2), 425−431.
(93) Chen, C.-C.; Huang, S.-H. The Effects of Particle Charge on the Performance of a Filtering Facepiece. *Am. Ind. Hyg. Assoc. J.* **1998**, *59* (4), 227−233.
(94) Moyer, E. S.; Stevens, G. A. "Worst-Case" Aerosol Testing Parameters: III. Initial Penetration of Charged and Neutralized Lead Fume and Silica Dust Aerosols through Clean, Unloaded Respirator Filters. *Am. Ind. Hyg. Assoc. J.* **1989**, *50* (5), 271−274.
(95) Hoppel, W. A.; Frick, G. M. The Nonequilibrium Character of the Aerosol Charge Distributions Produced by Neutralizes. *Aerosol Sci. Technol.* **1990**, *12* (3), 471−496.
(96) Davies, C. N. The Separation of Airborne Dust and Particles. *P. I. Mech. Eng.* **1953**, *167* (1b), 185−213.
(97) Payet, S.; Boulaud, D.; Madelaine, G.; Renoux, A. Penetration and Pressure Drop of A HEPA Filter during Loading with Submicron Liquid Particles. *J. Aerosol Sci.* **1992**, *23* (7), 723−735.
(98) Yeom, B. Y.; Pourdeyhimi, B. Aerosol Filtration Properties of PA6/PE Islands-in-the-Sea Bicomponent Spunbond Web Fibrillated by High-Pressure Water Jets. *J. Mater. Sci.* **2011**, *46* (17), 5761−5767.
(99) Eninger, R. M.; Honda, T.; Adhikari, A.; Heinonen-Tanski, H.; Reponen, T.; Grinshpun, S. A. Filter Performance of N99 and N95 Facepiece Respirators Against Viruses and Ultrafine Particles. *Ann. Occup. Hyg.* **2008**, *52* (5), 385−396.
(100) Montgomery, J. F.; Green, S. I.; Rogak, S. N. Impact of Relative Humidity on HVAC Filters Loaded with Hygroscopic and Non-Hygroscopic Particles. *Aerosol Sci. Technol.* **2015**, *49* (5), 322−331.
(101) Miguel, A. F. Effect of Air Humidity on the Evolution of Permeability and Performance of A Fibrous Filter during Loading with Hygroscopic and Non-Hygroscopic Particles. *J. Aerosol Sci.* **2003**, *34* (6), 783−799.

https://doi.org/10.1021/acsenvironau.1c00047
ACS Environ. Au 2022, 2, 290−309

(102) Gupta, A.; Novick, V. J.; Biswas, P.; Monson, P. R. Effect of Humidity and Particle Hygroscopicity on the Mass Loading Capacity of High Efficiency Particulate Air (HEPA) Filters. *Aerosol Sci. Technol.* **1993**, *19* (1), 94−107.
(103) Kim, C. S.; Bao, L.; Okuyama, K.; Shimada, M.; Niinuma, H. Filtration Efficiency of A Fibrous Filter for Nanoparticles. *J. Nanopart. Res.* **2006**, *8* (2), 215−21.
(104) Xu, B.; Wu, Y.; Lin, Z.; Chen, Z. Investigation of Air Humidity Affecting Filtration Efficiency and Pressure Drop of Vehicle Cabin Air Filters. *Aerosol Air Qual. Res.* **2014**, *14* (3), 1066−1073.
(105) Wang, L.-Y.; Yu, L. E.; Chung, T.-S. Effects of Relative Humidity, Particle Hygroscopicity, and Filter Hydrophilicity on Filtration Performance of Hollow Fiber Air Filters. *J. Membr. Sci.* **2020**, *595*, 117561.
(106) Mansour, E.; Vishinkin, R.; Rihet, S.; Saliba, W.; Fish, F.; Sarfati, P.; Haick, H. Measurement of Temperature and Relative Humidity in Exhaled Breath. *Sens. Actuators B Chem.* **2020**, *304*, 127371.
(107) US EPA, O. Mold Course Chapter 2: https://www.epa.gov/mold/mold-course-chapter-2.
(108) Konda, A.; Prakash, A.; Moss, G. A.; Schmoldt, M.; Grant, G. D.; Guha, S. Aerosol Filtration Efficiency of Common Fabrics Used in Respiratory Cloth Masks. *ACS Nano* **2020**, *14* (5), 6339−6347.
(109) van der Sande, M.; Teunis, P.; Sabel, R. Professional and Home-Made Face Masks Reduce Exposure to Respiratory Infections among the General Population. *PLoS One* **2008**, *3* (7), e2618.
(110) Ortiz, M. A.; Ghasemieshkaftaki, M.; Bluyssen, P. M. Testing of Outward Leakage of Different Types of Masks with A Breathing Manikin Head, Ultraviolet Light and Coloured Water Mist. *Intell. Build. Int.* **2021**, 1−19.
(111) Pan, J.; Harb, C.; Leng, W.; Marr, L. C. Inward and Outward Effectiveness of Cloth Masks, A Surgical Mask, and A Face Shield. *Aerosol Sci. Technol.* **2021**, *55* (6), 718−733.
(112) Mainelis, G. Bioaerosol Sampling: Classical Approaches, Advances, and Perspectives. *Aerosol Sci. Technol.* **2020**, *54* (5), 496−519.
(113) Wang, C.-H.; Chen, B. T.; Han, B.-C.; Liu, A. C.-Y.; Hung, P.-C.; Chen, C.-Y.; Chao, H. J. Field Evaluation of Personal Sampling Methods for Multiple Bioaerosols. *PLoS One* **2015**, *10* (3), e0120308.
(114) Clark Burton, N.; Adhikari, A.; Grinshpun, S. A.; Hornung, R.; Reponen, T. The Effect of Filter Material on Bioaerosol Collection of *Bacillus Subtilis* Spores Used as a *Bacillus Anthracis* Simulant. *J. Environ. Monit.* **2005**, *7* (5), 475−480.
(115) Burton, N. C.; Grinshpun, S. A.; Reponen, T. Physical Collection Efficiency of Filter Materials for Bacteria and Viruses. *Ann. Occup. Hyg.* **2007**, *51* (2), 143−151.
(116) Pan, M.; Lednicky, J. a.; Wu, C.-Y. Collection, Particle Sizing and Detection of Airborne Viruses. *J. Appl. Microbiol.* **2019**, *127* (6), 1596−1611.
(117) Jin, L.; Griffith, S. M.; Sun, Z.; Yu, J. Z.; Chan, W. On the Flip Side of Mask Wearing: Increased Exposure to Volatile Organic Compounds and A Risk-Reducing Solution. *Environ. Sci. Technol.* **2021**, *55* (20), 14095−14104.
(118) Scailteur, V.; Lauwerys, R. R. Dimethylformamide (DMF) Hepatotoxicity. *Toxicology* **1987**, *43* (3), 231−238.
(119) Xu, E. G.; Ren, Z. J. Preventing Masks from Becoming the Next Plastic Problem. *Front. Environ. Sci. Eng.* **2021**, *15* (6), 125.
(120) Zhang, B.; Zhang, Z.-G.; Yan, X.; Wang, X.-X.; Zhao, H.; Guo, J.; Feng, J.-Y.; Long, Y.-Z. Chitosan Nanostructures by *in Situ* Electrospinning for High-Efficiency PM2.5 Capture. *Nanoscale* **2017**, *9* (12), 4154−4161.
(121) Pakravan, M.; Heuzey, M.-C.; Ajji, A. A Fundamental Study of Chitosan/PEO Electrospinning. *Polymer* **2011**, *52* (21), 4813−4824.
(122) Li, L.; Hsieh, Y.-L. Ultra-Fine Polyelectrolyte Hydrogel Fibres from Poly(Acrylic Acid)/Poly(Vinyl Alcohol). *Nanotechnology* **2005**, *16* (12), 2852−2860.
(123) Brown, T. D.; Dalton, P. D.; Hutmacher, D. W. Melt Electrospinning Today: An Opportune Time for An Emerging Polymer Process. *Prog. Polym. Sci.* **2016**, *56*, 116−166.
(124) Buivydiene, D.; Krugly, E.; Ciuzas, D.; Tichonovas, M.; Kliucininkas, L.; Martuzevicius, D. Formation and Characterisation of Air Filter Material Printed by Melt Electrospinning. *J. Aerosol Sci.* **2019**, *131*, 48−63.
(125) Pai, C.-L.; Boyce, M. C.; Rutledge, G. C. On the Importance of Fiber Curvature to the Elastic Moduli of Electrospun Nonwoven Fiber Meshes. *Polymer* **2011**, *52* (26), 6126−6133.
(126) Croisier, F.; Duwez, A.-S.; Jérôme, C.; Léonard, A. F.; van der Werf, K. O.; Dijkstra, P. J.; Bennink, M. L. Mechanical Testing of Electrospun PCL Fibers. *Acta Biomater.* **2012**, *8* (1), 218−224.
(127) Huang, L.; Arena, J. T.; Manickam, S. S.; Jiang, X.; Willis, B. G.; McCutcheon, J. R. Improved Mechanical Properties and Hydrophilicity of Electrospun Nanofiber Membranes for Filtration Applications by Dopamine Modification. *J. Membr. Sci.* **2014**, *460*, 241−249.
(128) Choi, S.-S.; Lee, Y. S.; Joo, C. W.; Lee, S. G.; Park, J. K.; Han, K.-S. Electrospun PVDF Nanofiber Web as Polymer Electrolyte or Separator. *Electrochim. Acta* **2004**, *50* (2), 339−343.
(129) Rianjanu, A.; Kusumaatmaja, A.; Suyono, E. A.; Triyana, K. Solvent Vapor Treatment Improves Mechanical Strength of Electrospun Polyvinyl Alcohol Nanofibers. *Heliyon* **2018**, *4* (4), e00592.
(130) Mack, J. J.; Viculis, L. M.; Ali, A.; Luoh, R.; Yang, G.; Hahn, H. T.; Ko, F. K.; Kaner, R. B. Graphite Nanoplatelet Reinforcement of Electrospun Polyacrylonitrile Nanofibers. *Adv. Mater.* **2005**, *17* (1), 77−80.
(131) Wibisono, Y.; Fadila, C. R.; Saiful, S.; Bilad, M. R. Facile Approaches of Polymeric Face Masks Reuse and Reinforcements for Micro-Aerosol Droplets and Viruses Filtration: A Review. *Polymers* **2020**, *12* (11), 2516.
(132) Chen, R.; Wan, Y.; Wu, W.; Yang, C.; He, J.-H.; Cheng, J.; Jetter, R.; Ko, F. K.; Chen, Y. A Lotus Effect-Inspired Flexible and Breathable Membrane with Hierarchical Electrospinning Micro/Nanofibers and ZnO Nanowires. *Mater. Des.* **2019**, *162*, 246−248.
(133) Wang, N.; Cai, M.; Yang, X.; Yang, Y. Electret Nanofibrous Membrane with Enhanced Filtration Performance and Wearing Comfortability for Face Mask. J. *Colloid Interface Sci.* **2018**, *530*, 695−703.
(134) Li, Q.; Yin, Y.; Cao, D.; Wang, Y.; Luan, P.; Sun, X.; Liang, W.; Zhu, H. Photocatalytic Rejuvenation Enabled Self-Sanitizing, Reusable, and Biodegradable Masks against COVID-19. *ACS Nano* **2021**, *15* (7), 11992−12005.
(135) Zhang, S.; Liu, H.; Tang, N.; Zhou, S.; Yu, J.; Ding, B. Spider-Web-Inspired $PM_{0.3}$ Filters Based on Self-Sustained Electrostatic Nanostructured Networks. *Adv. Mater.* **2020**, *32* (29), 2002361.
(136) Liu, G.; Nie, J.; Han, C.; Jiang, T.; Yang, Z.; Pang, Y.; Xu, L.; Guo, T.; Bu, T.; Zhang, C.; Wang, Z. L. Self-Powered Electrostatic Adsorption Face Mask Based on A Triboelectric Nanogenerator. *ACS Appl. Mater. Interfaces* **2018**, *10* (8), 7126−7133.
(137) Senecal, A. G.; Senecal, K. J.; Magnone, J. P.; Pivarnik, P. E. Development of Nanofibrous Membranes towards Biological Sensing. In *Transformational Science and Technology for the Current and Future Force*; Selected Topics in Electronics and Systems; World Scientific, 2006; Vol. *42*, pp 387−393.

https://doi.org/10.1021/acsenvironau.1c00047
ACS Environ. Au 2022, 2, 290−309